ADDIS ABABA UNIVERSITY

SCHOOL OF GRADUATE STUDIES

DEPARTMENT OF EARTHSCIENCES

GEOPHYSICAL INVESTIGATIONS OF THE GERGEDI THERMAL SPRINGS, NORTH WEST OF WONJI, MAIN ETHIOPIAN RIFT

A THESIS SUBMITTED TO THE SCHOOL OF GRADUATE STUDIES OF ADDIS ABABA UNIVERSITY IN PARTIAL FULFILMENT OF THE REQUIREMENTS FOR THE DEGREE OF MASTER OF SCIENCE IN EXPLORATION GEOPHYSICS

BY

YAHYA ALI

JUNE, 2011

Addis Ababa University

School of Graduate Studies

College of Natural Science

Department of Earth Sciences

GEOPHYSICAL INVESTIGATIONS OF THE GERGEDI THERMAL SPRINGS, NORTH WEST OF WONJI, MAIN ETHIPIAN RIFT

BY
YAHYA ALI

JUNE, 2011

Approval by Board of Examiners

Dr. Tigistu Haile________________________________
Chairman, Department of Earth Sciences

Dr. Tigistu Haile ________________________________
Advisor

____
Examiner

____
Examiner

ACKNOWLEDGMENT

Firstly, I am indeed grateful to the Almighty for the sustenance, strength to the successful completion of my Msc program.

My profound gratitude goes to my Advisor Dr Tigistu Haile, for the proper supervision, support and guidance he provided me throughout my research. His critical Comments, Fatherly approach and unreserved effort have given me the opportunity to explore more. Besides the academics I have shared your way of positive approach to challenges either social or academics. Sincerely I appreciate your patience and willingness to devote much of your time and energy at all stages of my work.

Undoubtedly, my unreserved gratitude goes to my sweetheart Seada Mohammed, for her patience support and appreciation during my Msc program. I am highly indebted to my family for their support.

To all my instructors and colleagues in the department of Earth science and physics, I say thank you.

ABSTRACT

2D electrical resistivity imaging and total field magnetic surveys were carried out at Gergedi Thermal springs, located northwest of Wonji, in the Main Ethiopian Rift, with the aim of characterizing the thermal setting of the area. The area is geologically characterized by alluvial and lacostrine deposits, basaltic lava, ignimbrites and rhyolites and hydrogeologically all potential aquifers of low moderate and high permeability groups are present in the area. The prominent structural feature in the Rift, the SW to NE trending structures of the Wonji Fault Belt System, crosses over the study area.

Three traverse lines of imaging data, encompassing the active thermal springs, and about 500 magnetic data, covering the area with random distribution, were collected. From the analysis of the electrical survey data it is observed that the area is covered by low resistivity response region at shallow depths which is believed to result from saline moisturized soil subsurface horizon. Relatively medium and high resistivity responses subjected to weathered basalt, rhyolites and ignimbrites are also mapped. The electrical survey and the magnetic profiles have also indicated the presence of structures in most part oriented following the main structural units of the Wonji Fault System. The magnetic data have been qualitatively interpreted to show the presence of structures, which could act as paths for heat and fluids for the manifested springs, and to characterize the degree of thermal alteration of the area.

Results from these investigations suggest that the Gergedi thermal springs area are controlled by fault systems oriented parallel and sub parallel to the main tectonic lines of the Rift and potential sites of shallow thermal water resource, other than the current active thermal springs, are also detected that can be used for further exploitation of the resource.

TABLE OF CONTENTS

List of Figures

LIST OF TABLES

ACRONYMS

1D-One Dimension

2D-Two Dimension

3D-Three Dimension

CVES-Continuous Vertical Electrical Sounding

EARS-East African Rift System

ELC-Electro Consult

EMR-Ethiopian Main Rift

ERT-Electrical Resistivity Tomography

GPS-Global Positioning System

IGRF-International Geomagnetic Reference Field

RMS-Root Mean Square

RTP -Reduction To Pole

UTM-Universal Transverse Mercator

VES-Vertical Electrical Sounding

WFB-Wonji Fault Belt

WGS-World Geodetic System

CHAPTER ONE

INTRODUCTION

1.1 General

The discipline geophysics applies the principles of physics for the investigations of the interior of the Earth. It involves taking measurements at or near the Earth's surface that is influenced by the internal variation in physical properties. Analysis of these measurements can reveal how the physical properties of rocks comprising the Earth's interior vary vertically and laterally.

Geophysical methods play a key role in geothermal exploration since many objectives of geothermal exploration can be achieved by these methods. The geophysical surveys are directed at obtaining indirectly, from the surface or from shallow depth, the physical parameter of the geothermal system.

1.2 Overview of Geothermal System: Process, Model and Geology

Geothermal energy can be expressed as the heat generated within the Earth which could be exploited for different use according to the amount of temperature that is produced. Geothermal resources, according to Mary and Mario (2004), are generally associated with tectonically active regions which are generated as a result of plate movements and volcanic activities that result in temperature differences between the different parts of the asthenosphere where convective movements are formed. This slow convective movement is said to be maintained by the radioactive elements and heat from the deepest part of the Earth. The less dense, deep hotter rocks tends to rise along with the movement towards the surface while the colder but heavier rocks close to the surface tend to sink, re-heat and rise again. Figure (1.1) shows an ideal model of a geothermal system.

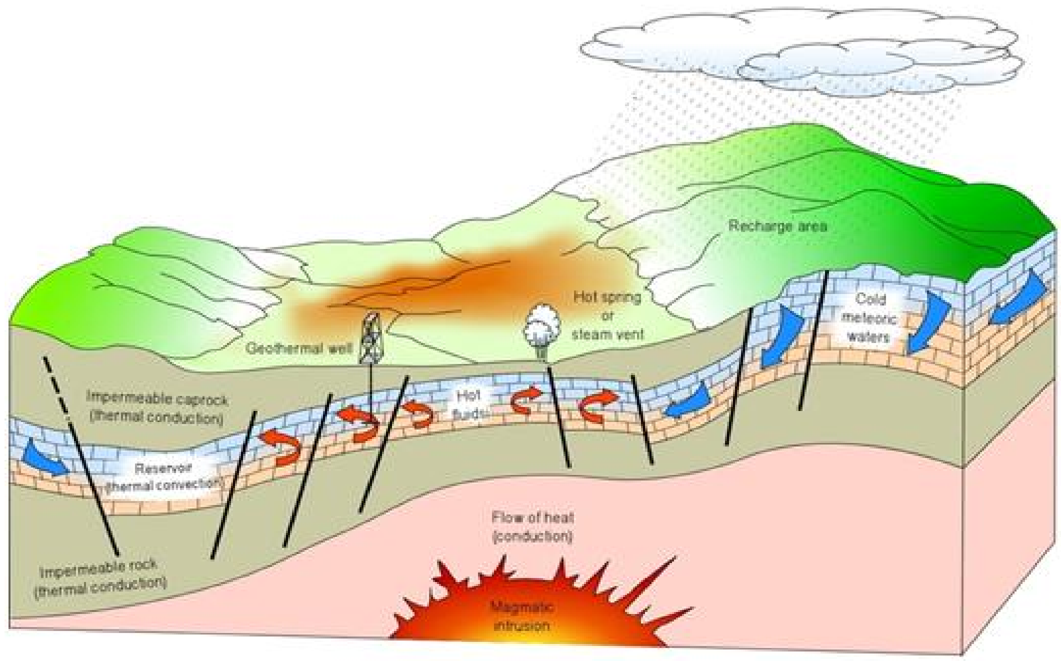

Figure 1.1 Schematic representation of an ideal geothermal system (after Mary and Mario,2004).

Geothermal resource refers to the thermal energy stored in the Earth's crust. Thermal energy in the Earth is distributed between the constituent host rock and the natural fluid possibly contained in its fractures and pores at temperatures above ambient levels.

A geothermal system is made up of four main elements: a heat source, a reservoir, a fluid, which is the carrier that transfers the heat, and a recharge area. The heat source is generally a shallow magmatic body, usually cooling and often still partially molten. The volume of rocks from which heat can be extracted is called the geothermal reservoir-a summary term describing hot water, vapor and gases-which contains hot fluids. A geothermal reservoir is usually surrounded by colder rocks that are hydraulically connected with the reservoir. Hence, water may move from colder rocks outside the reservoir (recharge) towards the reservoir where hot fluids move under the influence of buoyancy forces towards a discharge area.

Geothermal energy is the natural heat of the Earth. The thinned and fractured crust allows the magma to rise to the surface as lava. The greatest part of the magma does not reach the surface but heats large regions of underground rocks. Rainwater can seep down the faults and fractured rocks for miles. After being heated, it can return to the surface as steam or hot water. When hot water and steam reach the surface, they can form fumaroles, hot springs, mud pots and other interesting phenomena. Otherwise, when the rising hot water and steam is trapped in permeable and porous rocks under a layer of impermeable rock, it can form a geothermal reservoir, which could be a powerful source of energy. This clean renewable energy can be used in many areas like the Ethiopian Rift, where the geological situations favor the availability of the resource.

Geothermal resources vary widely from one location to another, depending on the temperature and depth of the resource, the rock chemistry and the abundance of ground water. Geothermal resources are predominantly of two types: high temperature such as found in volcanic regions and island chains, and moderate to-low temperature that are usually found extensively in most continental areas.

The type of geothermal resource determines the method of its utilization. High-temperature resources (dry steam/hot fluids) can be gainfully utilized to generate electric power, whereas the moderate-to-low-temperature resources (warm to hot water) are best suited for direct uses. However, aided by modern technology, even the moderate temperature resources are being utilized for generation of electric power using the binary-cycle method.

Geological setting in which a geothermal reservoir is to be found can vary widely. The largest geothermal fields currently under exploitation occur in rocks that range from limestone to shale, volcanic rock and granite. Volcanic rocks are probably the most common single rock type in which reservoirs occur. Rather than being identified with a specific lithology, geothermal reservoirs are more closely associated with heat flow systems. Many of the developed geothermal reservoirs around the world occur in convection systems in which hot water rises from deep within the earth and is trapped in reservoirs whose cap rock has been formed by silicification, or precipitation of other mineral elements. As far as geology is concerned, therefore, the important factors in identifying a geotherma1 reservoir are not rock units, but rather the existence of tectonic elements such as fracturing, and the presence of high heat flow. The high heat flow conditions that give rise to geothermal systems commonly occur in rift zones, subduction zones and mantle plumes, where, for unknown reasons, large quantities of heat are transported from the mantle to the crust of the earth.

Geothermal energy can also occur in areas where thick blankets of thermally insulating sediment cover basement rock that has a relatively normal heat flow. Geothermal systems based on the thermal blanket model are generally of lower grade than those of volcanic origin.

An important element in any model of a geothermal system in a volcanic area is the source for the system: in other words, the existence of an intruded hot rock mass beneath the area where the shallower reservoirs are expected to occur. The source of a geothermal system could be either a pluton or a complex of dykes, depending upon the rock type injected.

1.3 Geothermal Studies in Ethiopia

Ethiopia launched a long-term geothermal exploration undertaking in 1969. Over the years, a good inventory of the potential target areas has been built up and about 16 geothermal prospects (Figure 1.2) are judged as having potential for electricity generation (Meseret Teklemariam,et al., 2000).These works were aimed at studying the geology, geochemistry and hydrology of hot springs of the section of the East African Rift system within Ethiopia.

According to the Ethiopian Electric Power Corporation, geothermal energy development is second in priority to hydropower. Feasibility studies had confirmed that Ethiopia has a potential of 5,000MWE of geothermal resources in the Ethiopian rift valley. However, the initial investment for a geothermal energy plant is huge and also the risk is relatively high (the excavation of expensive wells frequently fails). Therefore, no big plant has been built for more than 10 years after the first pilot plant at Alto-Langano was established. The identified potential areas for geothermal energy plants are (Figure 1.2); I) lakeside areas, such as Alto-Langano, Corbetti and Abaya, ii) South Afar area, such as Tulu-Moye, Gedemsa, and Dofan, and iii) North Afar area, such as Tendaho and Dallol. (Meseret Teklemariam,et al., 2000)

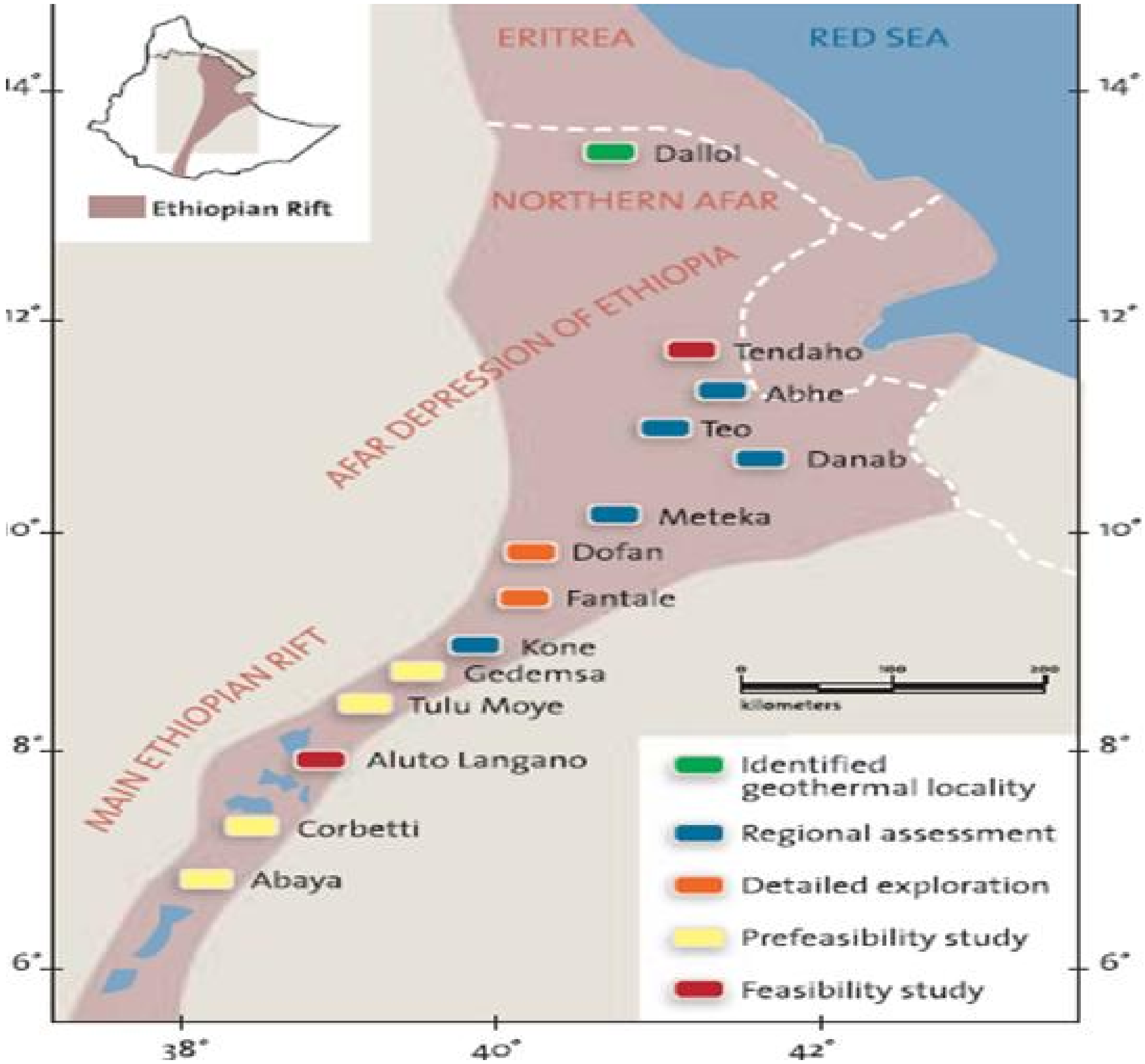

Figure 1.2 Location map of the geothermal prospect areas within the Ethiopian Rift Valley (after Meseret Teklemariam, 2000)

1.4 Reviews of previous studies

A large number of publications on the geology, volcano-tectonic development, hydrogeology and some on geophysical studies of the Main Ethiopian Rift in general, on the central sector in particular, have been produced in the past. Revising these studies will help to understand the regional geology and hydrogeology of the study area. Thus, in this part some of the regional and local studies have been revised and presented.

Electro Consult (ELC) with Geothermica Italiana and the Ethiopian Institute of Geological Surveys jointly carried out a study during the year 1985-1987 under the project entitled

“Geothermal Reconnaissance study of selected sites of the Ethiopian Rift System”. The purpose of the survey was to identify target areas for future detailed study to be carried out. With this aim, Gedemsa area was selected as one of the promising geothermal prospects in the Main Ethiopian Rift Valley.

Integrated geophysical investigation to study thermal zones at Boku volcanic center were carried out by Tigistu Haile et al., (2002).the study concluded that the Boku thermal field is a vapour dominated, dry type geothermal system tapping heat from the shallow acidic magma chamber of Quaternary volcanic rocks of the rift floor. The study also showed that the Quaternary faults are the major tectonic structures for the passage of the deep seated vapor to the surface and the recharging of the geothermal reservoir.

Tamiru Alemayehu and Vernier (1997) have undertaken a research over Boku with a title “Conceptual model for Boku hydrothermal area”. As indicated in the study, the geothermal fluids in the Boku area come to the surface along deep fractures. It is also stated in the paper that the geothermal gradients around Nazareth are very high as indicated by higher shallow ground water temperature (=26^0C) which could be due to the presence of shallow depth circulation of thermal waters that rise to these depths through the structures that resulted from the past intense tectonic and volcanic activities.

Tamiru Alemayehu and Tigistu Haile, (2008) studied the Boku thermal area using geophysical methods. Their study also suggests that the Boku area is characterized by deep running faults and a thermal reservoir that probably receives recharge from multiple sources, but mainly from the regional groundwater system. The main conduits for the thermal recharge from deep-seated thermal sources are probably the Quaternary faults and fractures.

Theodros Solomon (2008) for his Msc thesis did research over the Gergedi Thermal Springs using integrated geophysical investigation methods namely gravity and vertical electrical sounding (VES).The paper concluded that the main sources of heat for the springs is not underneath the spring, it is indicated in the paper as well that the most probable source is the neighboring Gedemsa Caldera, faults are the main conduits for the recharge of heat and water for the spring.

Aquifer characteristics of the Gergedi thermal springs were studied by Tigistu Haile and Tamiru Alemayehu (2010). From the study, the heat sources are potentially derived from the collapsed Gedemsa caldera and the recharging water that feed the large discharge springs come from fluids in deep circulation from the Koka reservoir.

1.5 Problem Statement

There are hot springs all over the Earth, on every continent and even under the oceans and seas. It is known that the temperature of rocks within the earth increases with depth. The rate of temperature increase with depth is known as the geothermal gradient. If water percolates deeply enough into the crust, it will be heated as it comes into contact with hot rocks. Due to buoyancy these heated water comes in to the surface and form hot springs.

Hot spring sites and their underneath geothermal groundwater system are valuable natural resources for geothermal utilization and tourism industry. Many such in Ethiopian Rift Valley provinces, such as Filwuha, Sodere, Langano, Weliso, and Wondo Genet have become well-known touristic spots and consequently play an important role in the local tourism industry. In contrast, the promising Gergedi Thermal springs with large volume of discharge, relatively hottest temperature, the nearest to the towns:- capital Addis Ababa, Nazareth, and Wonji is used traditionally for the medication purpose only, which currently is under exploited and under investigated. Hence there is a need for a detailed investigation of this area and assess its potential use through development of new areas of thermal water extraction.

Besides the mentioned economic significance, although there has been continued interest in the study of the nearby Gedemsa caldera, nowadays one rarely finds literature and material devoted to the study of this resource whose occurrence seems to be an integral part of the caldera itself. The large volume of discharge and its possible relation with the caldera and Lake Koka are interesting phenomena that further need a detailed investigation. In addition to the study of the relationship of the spring with these two features (Gedemsa caldera and Lake Koka), the form and morphology of the deeper heat sources, the depth to the potential aquifers, major structures in the area, the potential sources of discharge, its recharging mechanism, etc. need more work.

This research therefore employs the use of geophysical methods to understand the active tectonic lineaments (faults and fractures) on the hydrothermal springs around Gergedi and to characterize the thermal setting of the area.

1.6 Location and Geological setting of the study area

1.6.1 Location of the study area

The Gergedi thermal spring is the most commonly used and relatively well known thermal spring in Ethiopia, widely used for therapeutic and recreational purposes. The spring is located in the central part of the East African Rift System (EARS) and within the Main Ethiopian Rift close to the city centers of Nazareth and Wonji adjoining the Awash River, more specifically, about 130km, SE of Addis Ababa; 30Km, SW of Nazareth and 5km, north west of Wonji town. Figure (1.3) gives the general location of the survey area and the location of the thermal springs.

The study area, although highly localized to the areas of the thermal springs, is bounded between UTM coordinates (521010-522379) Easting and (935001-936704) Northing and covers approximately 15km^2 surface area with the center of the survey located in the regions of maximum manifestation of the thermal activities.

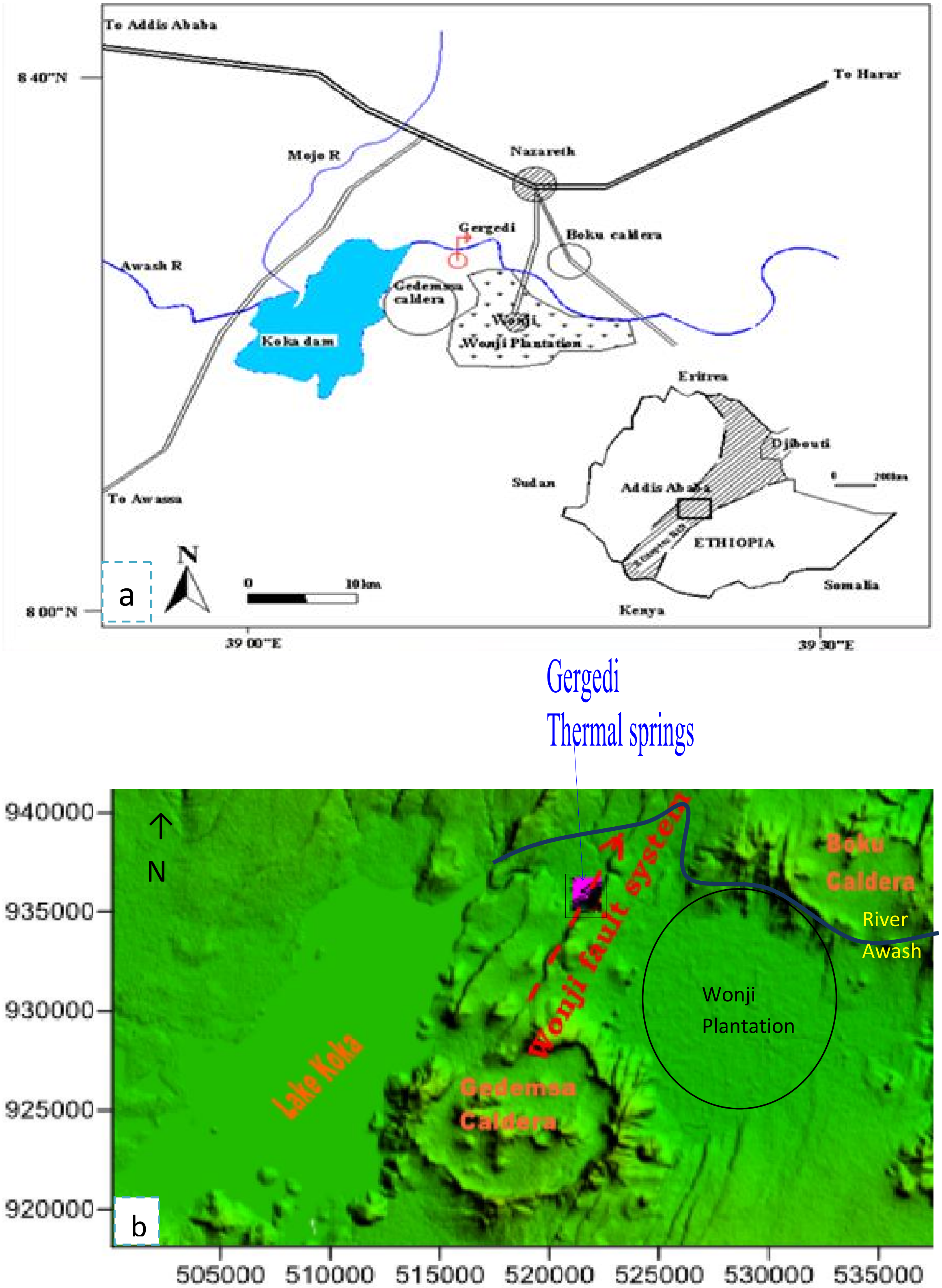

Figure 1.3 Location map of the study area (a) and the digital elevation model (DEM resolution 30m) around Gergedi Thermal Springs (b).

1.6.2 Tectonics of the Ethiopian Rift Valley

Separating the Ethiopian and Somalian plateaus, the Ethiopian Rift Valley (a part of the East African Rift Valley) is a relatively sunken, faulted zone, which runs generally in the SSW–NNE direction from Lake Turkana (formerly Lake Rudolf) to the Danakil triangle where the African Rift System joins the Red Sea and the Gulf of Aden Rifts. The northern part of the Afar Triangle is a topographically well defined depression, sharply limited on both sides by steep scarps of Paleozoic and Mesozoic origin: the Ethiopian escarpment to the west and the Danakil horst to the east, which runs parallel to the Red Sea coast of southern Eritrea. The Ethiopian Rift floor rises to a height of over 1800m at the watershed north of Lake Ziway and then descends northwards while spreading into wide plains and areas of which in the Danakil Depression are below sea level (Mohr, 1962).

Central Ethiopia is an area of complex geology and topography characterized by a narrow rift zone that separates the southwestern plateau from northwest plateau. The natural complexity of the area, its rugged topography and intensive volcanic and tectonic activity, give rise to different groups of springs, both gravity and non-gravity types (Tamiru Alemayehu, 2003).These surface manifestations overlie a highly modified deep lithospheric structure, but many questions about the structure and evolution of this rift zone remain unanswered (Nicolas et al., 2007).

Figure (1.4) shows structural sketch of part of the Main Ethiopian Rift containing the study area.

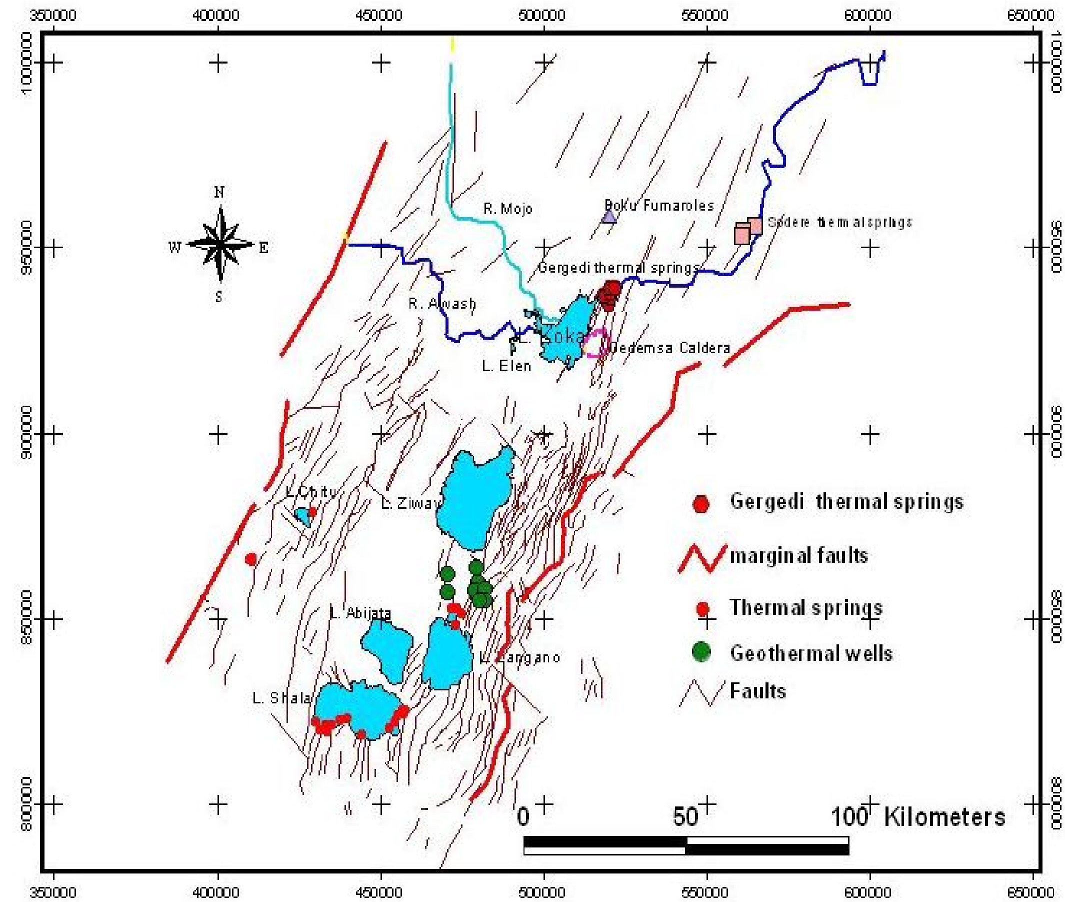

Figure 1.4 Structural map on the central Main Ethiopian Rift with the inset location of Koka-Wonji area (after Boccaletti M.,et al.,1998)

1.6.3 Geology of the Study Area

Being the region of intense tectonic activity, with crustal thinning, asthenosphere uplifting and associated volcanism, the MER is an area of a high thermal regional anomaly. The heat anomaly is further enhanced by magmatic processes such as those requiring a large volume of magma to be emplaced and differentiated at shallow depth in order to produce the corresponding voluminous silicic melts erupted at surface. In the study area, the rhyolitic volcanic complexes are considered to be products of these differentiated magmatic processes. The privileged thermal zones are, therefore, those corresponding to the large central volcanoes of Quaternary age, The WFB of the MER (Mohr, 1967)

More specifically, the study area is situated to south west of Adama town, especially between Lake Koka and the Wonji plantation, in the Main Ethiopian Rift. Numerous thermal springs of differing but relatively high temperature exists in the area. These thermal springs are manifestation of geothermal activity as a result of the phenomena related to the rift formation. Normal faults, which are parts of the Wonji Fault Belt system, and the Gedemsa caldera- which is considered as the sources of thermal energy of the hot springs in the Gergedi- are situated in the vicinity of the study area.

The major tectonic lines, which are aligned in NNE-SSW and NE-SW direction in the rift floor, form numerous local graben and horst structures (Rift-in-Rift structures).The axial part of the Rift is dominated by acidic volcanoes, which are rooted along these tectonic lines and are characterized by collapsed calderas; among which the Boku and the Gedemsa Caldera occupy the eastern and the south western part of the study area (Gergedi thermal springs) respectively (Figure 1.3 b).

A detailed geological map of the thermal springs area (study area) is given in Figure 1.5 The main lithologic units around the study area and the Boku and Gedemsa units are discussed in detail in the following sections.

The Eastern Margin of the Rift consists of ignimbrites and acidic lava flows, Dera-Nathareth unit composed of acidic lava flow and domes of ignimbrite and basalt. The Boku volcanic ridge is made of alkaline and peralkaline rhyolite lava domes and flows, aged about 0.8my (Alula Damte et al., 1992), which covers the floor complex ignimbrites in the central part of the rift. From stratigraphic point of view, the Boku rhyolites fall between the Adama-Boku basalt and the Wonji basalts, the acidic rock consisting of rhyolite lava domes, obsidian flows, tuffs and ashes.

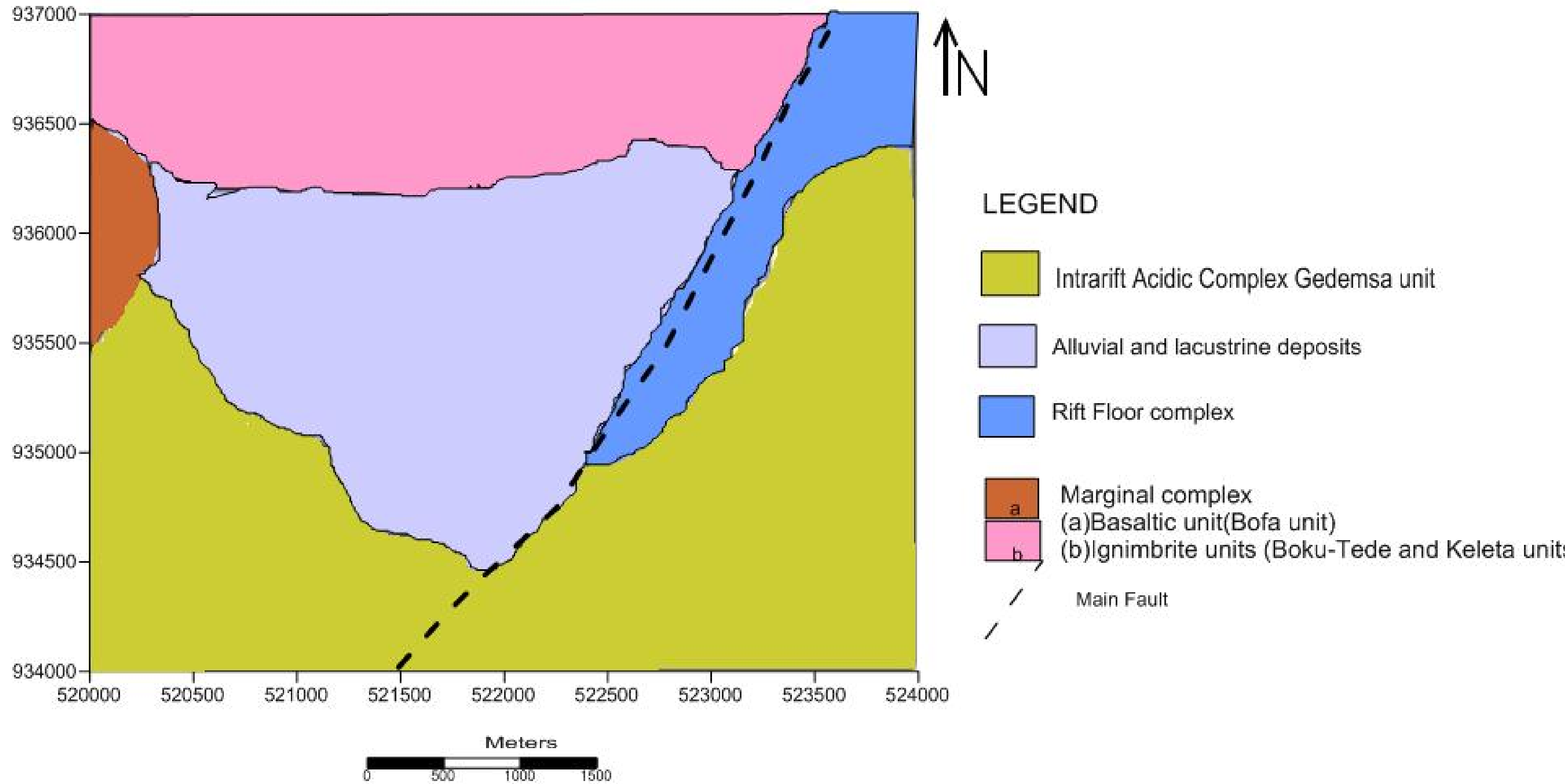

Figure 1.5 Geological map of the study Area (Modified frome Allula Damte et al., 1992).

Rocks of the Gedemsa unit on the other hand are associated with a central volcano that later collapsed and formed calderas. The Gedemsa caldera is well preserved to explain this event. This 8km wide and 0.83-0.2 km high caldera consists of pyroclastic flow ignimbrites, rhyolite, obsidian lava flows and pumice fall deposits stratified from bottom to top. This unit is characterized by felsic products related to the formation of a caldera (Gedemsa). The volcanic products from the caldera are predominantly acidic in nature and are dominated by ignimbrites associated with ash flows, pumice falls and surge deposits. The post caldera products are mainly rhyolitic lava flows. The Gedemsa volcano is cut by NE-SW trending faults of the Wonji Fault Belt. Basaltic activity connected to this fault system resulted in surge deposits, cinder cones and lava flows inside and outside the caldera. Peralkaline rhyolites and trachytes are by far the most abundant products. During and just after the volcanic activity that gave rise to the Gedemsa products, basaltic magmas were erupted in the area. Thus basaltic spatter and cinder cones are found both inside and on the caldera rims (Theodrose Solomon, 2008 and the reference therein).

The representative volcanic stratigraphy of the central part of the Main Ethiopian Rift as stated in Mohr (1983) is presented in Table 1.

Table 1.The Nazareth area volcanic stratigraphy (Mohr, 1983 and the reference therein; Alula Damte et al., 1992; Tamiru Alemayehu and Vernier, 2003).Quaternary=0-1.7 my Pliocene=1.7-5my

Age (millions years)	Main lithology	Thickness (meters)
0.25	Boseti and Gedemsa Basalts	≈3-4
	Unwelded ignimbrites	≈5
0.45-0.4	Bofa basalts(olivine basalts)	
0.5	Gedemsa ignimbrites	≈20-50
0.6	Adama-Boku basalts	≈5
0.8	Boku rhyolites	≈200
1.6	Wonji basalts	
1.7-1.6	Boseti ignimbrites/Floor complex ignimbrites	> 100
3.3-3.1	Tede rhyolites	

1.7 Hydrogeology of the Area

The Main Ethiopia Rift is characterized by many faults, and horsts and graben structures. According to Getaneh Kebede (1987), the Nazareth group ignimbrite shows variable pearmeability in different areas and is described by its jointed and faulted nature. Rocks occuring in the northeast of Melka Jilo and Koka areas have high permeability, consisting of many thermal springs having discharge capabilities ranging from 38 to 798 l/sec (Getaneh Kebede, 1987).

Numerous springs, dominantly warm springs, also occur downstream of Lake Koka that receive recharge from deep sources and the Koka reservoir through the NE-SW fault lines. The leakage of Koka reservoir through faults that feed springs located below the dam site has been widely reported. The large volume of water supply from the reservoir also has the effect of reducing the temperature of the thermal springs downstream (Tamiru Alemayehu, 2003).

Volcanic thermal springs are strictly associated with acidic volcanic centers that could have shallow magma chamber. Faults play an important role by acting as conduits to transport thermal water to the surface, even in this case, the additional recharging water comes from precipitation.

In the volcanic rocks (that predominantly occur over the study area) the occurrence of aquifers mainly depends on structures contained and processes that form these rocks. Volcanic rocks resulting from explosive magmatic activity, like pumice falls and scoria, for example, have very high intergranular permeability while in lava flows primary permeability is mainly due to vesicles and jointing at the time of flowing.

Based on the degree of weathering, fracturing and pore interconnection both consolidated and unconsolidated materials exposed in the area are categorized in to three main permeability groups, such as low, moderate and high permeable rocks.

Massive ignimbrites, rhyolitic lava flows and domes are low permeable rocks which do not posses sufficient fracture openings that could facilitate water infiltration and circulation (Theodros Solomon, 2008).

Rocks that are grouped under moderate permeability category include fractured ignimbrites, mixed pyroclastic deposits, slightly fractured basaltic lava flows. These rocks are characterized by sufficient amount of factures with measurable opening and spacing.

Scoria, alluvial deposits and highly fractured basaltic lava flows are included in highly permeable rocks. The alluvial deposits that are found along the Awash River and Wonji sugar plantation are productive aquifers since they posses sufficient interstitial porosity. In the study area, alluvial sediments are found along the river channels and are made of materials ranging from clays to gravel (Aula Damte et.al., 1992).

The discharge temperature of Gergedi thermal springs vary between 41°C and 47°C for those which are away from the Awash River. The spring located nearby the Awash River has a bit lower temperature (26°C-33°C) this is due to the cooling effect of the river (Theodrose Solomon, 2008 and the reference therein).

A number of studies have shown that the leakage of the Koka reservoir has been detected on the Gergedi springs. All existing cold and thermal springs are located along the tectonically active zones dominated by normal faults and extensional fractures (Theodros Solomon, 2008 and the references therein).

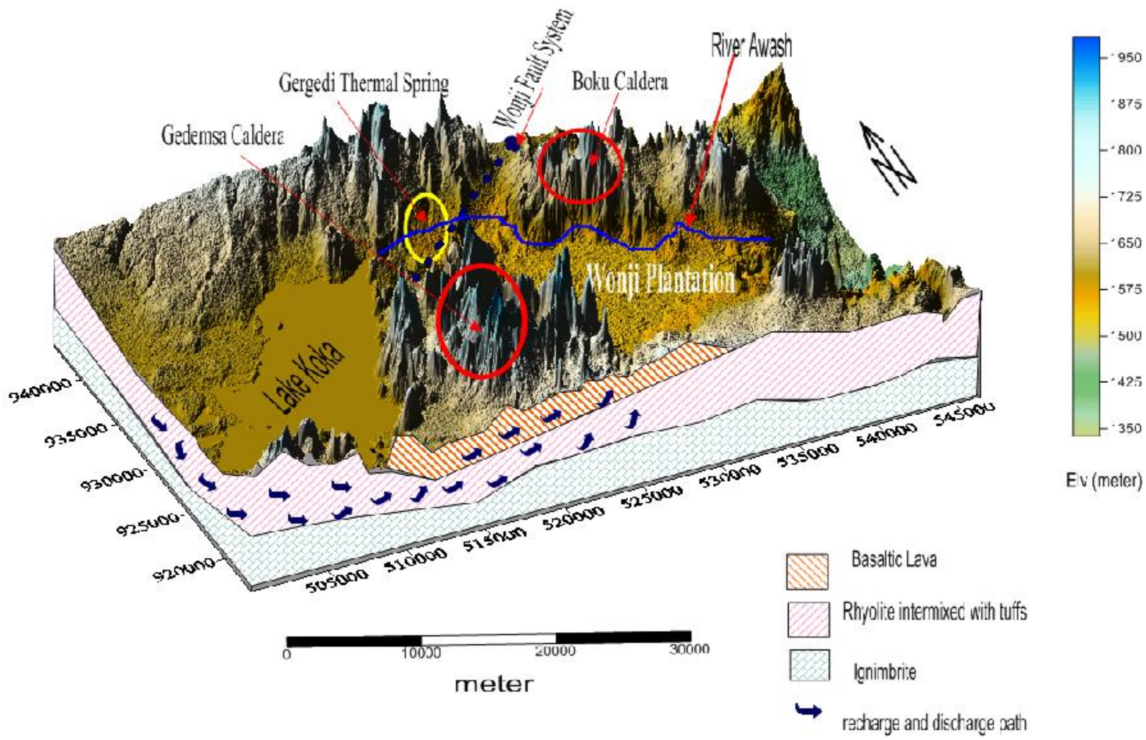

Figure 1.6 3D surface map of Digital Elevation Model showing conceptual model for the Gergedi thermal springs aquifer setting (modified after Tigistu Haile and Tamiru Alemayehu,2010).

1.8 Objectives of the Study

1.8.1 General Objective

The general objectives of this study are to characterize the thermal setting of the Gergedi Thermal springs area and to provide the necessary background information for further development of the thermal resources.

1.8.2 Specific objectives

- Mapping the major geologic structures over the area that act as paths for rising hot water and the recharging of the springs.
- Study the potential of the thermal springs for further development and delineate prospective areas for utilisation of the thermal springs from surface, near surface and

shallow depth discharges.

- Defining the major subsurface geoelectric units of the area around the springs and if possible determine the depth to the aquifers.
- Familiarizing oneself with practical methodologies of geophysical data acquisition, data analysis and interpretation.

1.9 Methodologies

Geophysical methods are applied in a wide variety of areas. They are used for oil and mineral prospecting, for solving groundwater, geothermal and engineering problems. Moreover, geophysics plays a fundamental role in studies of the Earth's deep interior otherwise inaccessible by other means.

In this study, an integrated geophysical methods namely magnetic and 2D resistivity imaging (electrical resistivity tomography) methods were selected and conducted to investigate the Gergedi thermal springs.

Magnetic surveys are commonly used exploration tools for their ability in lithologic differentiation of the basement and their ability to highlight structural features like faults, grabens and horsts. In geothermal exploration this technique is found to be even more attractive and of high potential, as it is suited for mapping hydrothermal alteration zones related to the presence of a geothermal reservoir and rising thermal fluids. These are often characterized by the alteration of magnetite to pyrite, and therefore give magnetic responses less than that of unaltered zones. And resistivity surveys in particular, on the other hand, can locate anomalies that are directly related to the presence of geothermal fluids. These and other field practice related advantages of the techniques led us to employing the methods at Gergedi thermal springs in this study.

To fulfill the objectives of the study mentioned above, various approaches have been used in the area of investigation. The first step was reviewing previous literatures for the understanding of the geology and hydrogeology of the study area .field work for, magnetic and electrical resistivity data collection, has been done. Finally using different software, the collected data have been processed and interpreted.

CHAPTER TWO

THEORY OF THE GEOPHYSICAL METHODS USED

2.1 The Direct Current Resistivity method

2.1.1 Introduction

Electrical methods of prospecting detect the surface effects produced by electric current flow in the ground. Using electrical methods, one may measure potentials, currents, and electromagnetic fields which occur naturally or are introduced artificially in the ground. In addition, the measurements can be made in a number of ways to arrive at a variety of results.

Direct Current resistivity methods are based on the injection of a current into the ground to measure the generated electrical field as a potential difference. The experimental configuration of the electric resistivity method consists of four electrodes: two of them are the current electrodes, AB, through which a current I (Amperes) is injected and the other two are the potential electrodes, MN, where a potential difference ΔV (Volts) is recorded. The ratio of voltage to current is the resistance that, when multiplied by a factor which takes into account the spacing between the electrodes, gives a parameter known as the apparent resistivity.

2.1.2 Fundamental principles of DC resistivity survey

The fundamental physical law used in resistivity surveys is the Ohm's law that governs the flow of current in the ground. The equation for Ohm's law in vector form for current flow in a continuous medium is given by

$$J = \sigma E \tag{2.1}$$

where $\boldsymbol{\sigma}$ is the conductivity of the medium, $\mathbf{J}$ is the current density and $\mathbf{E}$ is the electric field intensity. But practically what is measured is the electric potential, which is related with the electric field by the equation.

$$E = -\nabla . V \quad (2.2)$$

Combining the equations (1) and (2), we get

$$J = -\frac{1}{\rho}\nabla V, \text{ where } \sigma = \frac{1}{\rho} \quad (2.3)$$

where, **ρ** is resistivity- one of the most important variable of physical properties in nature. Generally, porosity is the major control of the resistivity of rocks and that resistivity generally increases as porosity decreases.

The geometrically-independent quantity that is used in direct current method is resistivity and is defined by considering a wire of length L, cross section area A and resistance of R as

$$\rho = \frac{RA}{L} \quad (2.4)$$

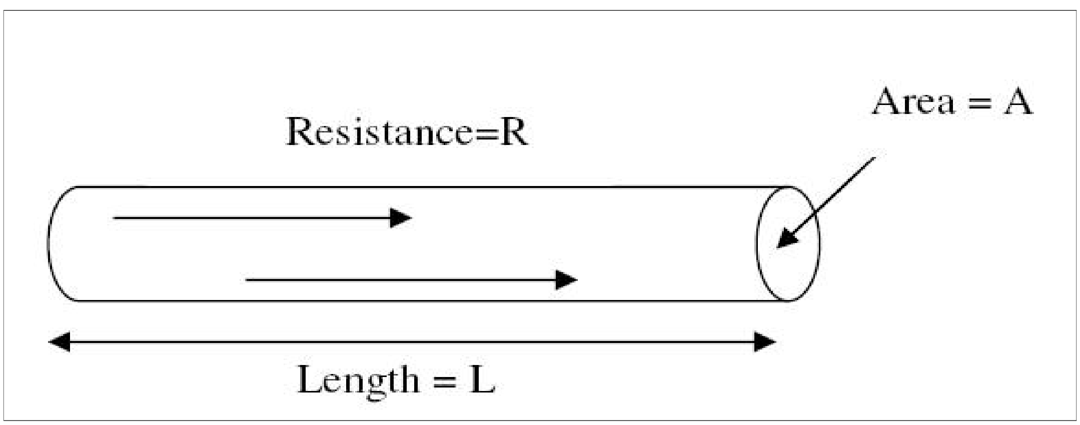

Figure 2.1 Parameters used in defining resistivity.

2.1.3 Resistivity of Earth Materials

All materials, including soil and rock, have an intrinsic property, resistivity, which governs the relation between the current density and the gradient of the electrical potential. Variations in the resistivity of earth materials, either vertically or laterally, produce variations in the relations between the applied current and the potential distribution as measured on the surface, or thereby reveal something about the composition, extent, and physical properties of the subsurface materials. And therefore Resistivity is one of the most variable of physical properties. Certain minerals such as native metals and graphite conduct electricity via the passage of electrons.

Most rock-forming minerals are, however, insulators and electrical current is carried through them is mainly by the passage of ions in pore waters. Thus, most rocks conduct electricity by electrolytic rather than electronic processes. It follows that porosity is the major control of the resistivity of rocks, and that resistivity generally increases as porosity decreases. However, even crystalline rocks with negligible intergranular porosity are conductive along cracks and fissures. Figure (2.2) shows the range of resistivity expected for common rock types. It is apparent that there is considerable overlap between different rock types and, consequently, identification of a rock type is not possible solely on the basis of resistivity data.

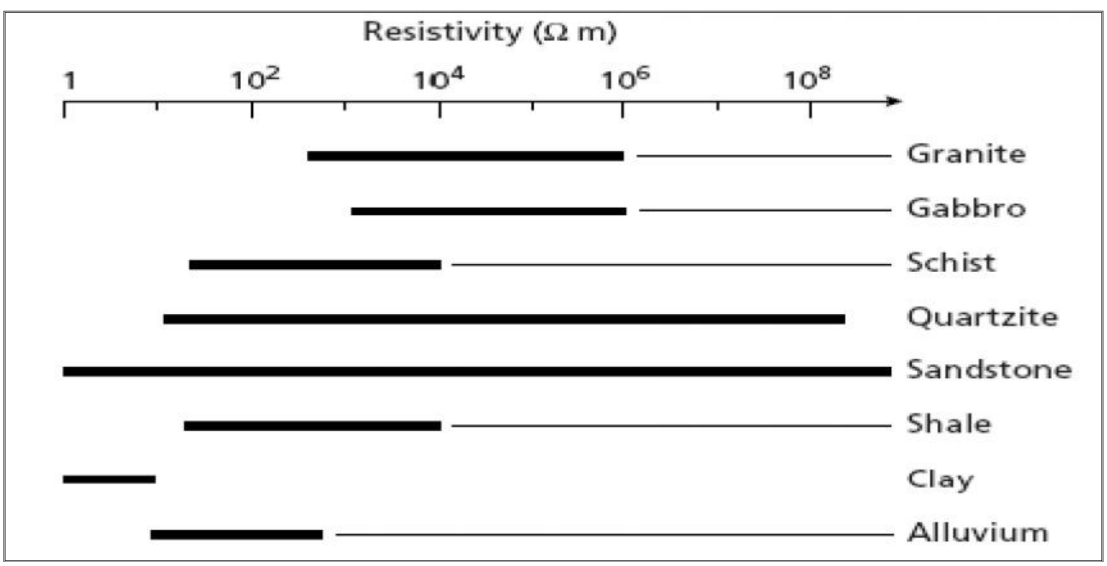

Figure 2.2 Resistivity of common rocks.

There is a large range of resistivity, not only between varying rocks and minerals but also within rocks of the same type. This range of resistivity, as described above, is primarily a function of fluid content. Thus, a common target for electrical surveys is the identification of fluid saturated zones. For example, resistivity methods are commonly used in engineering and environmental studies for the identification of the water table.

In groundwater based investigations, the resistivity of water-saturated ground show a very large variations. Altered rock and saturated horizon/aquifer resistivity is determined by the kind of water they hold. The resistivity of water and groundwater associated rocks and their relationships can be presented in a form of resistivity scale as in the following Table 2.

Table 2.Resistivity scale for water and water-rock formations.

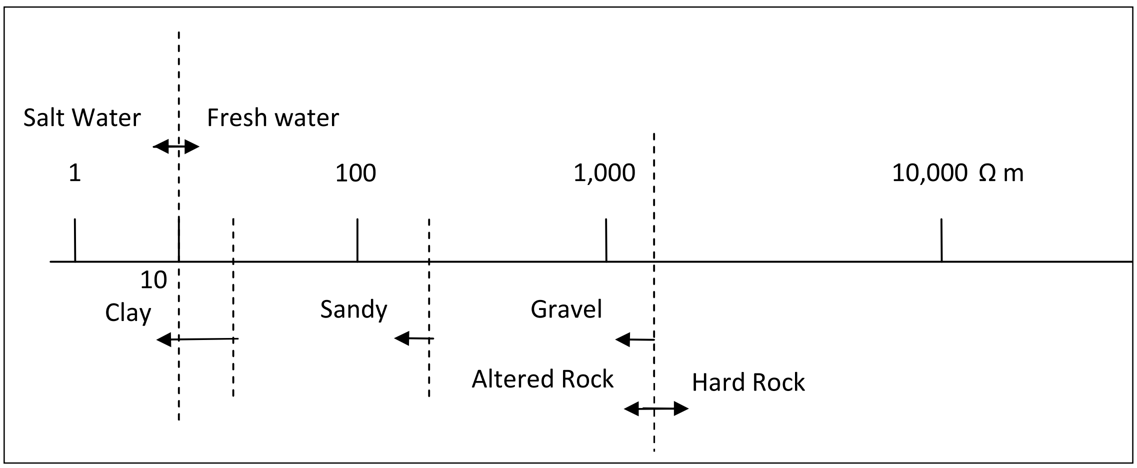

2.1.4 Apparent resistivity

Consider the case where the current sink is at an infinite distance from the source (Figure 2.3).The potential V_C at an internal electrode **C** is the sum of the potential contributions V_A and V_B from the current source at **A** and the sink at **B,** and can be given by

$$V_C = V_A - V_B \quad (2.5)$$

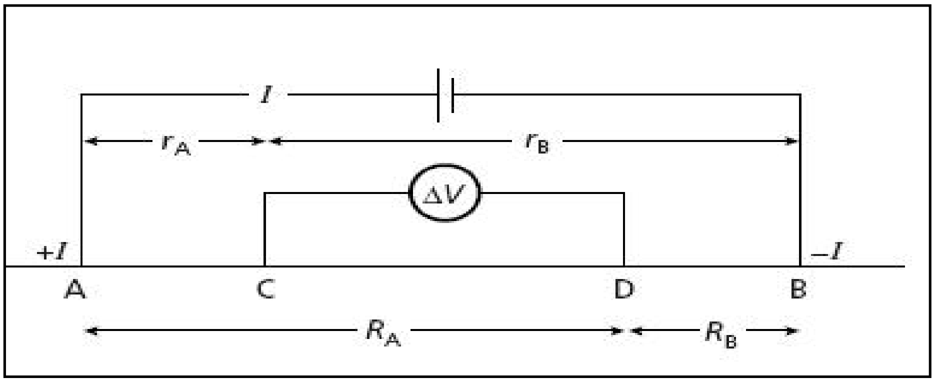

Figure2.3 The generalized form of electrode configuration used in the resistivity survey.

Now consider the case where the above electrode layout is placed over a homogeneous ground, the potential difference measured depends on the current applied, the resistivity of the subsurface medium and the geometric factor (k) determined by the array configuration (distance between electrodes).

$$\Delta V = Vc - V_D = \frac{I\rho}{2\pi}\left(\frac{1}{r_1} - \frac{1}{r_2} - \frac{1}{r_3} + \frac{1}{r_4}\right) \tag{2.6}$$

It is clear that the resistivity determined using equation (2.13) is a function of the electrical parameters of the subsurface and the geometry of the disposition of the electrodes, and is not a constant. This resistivity is called apparent resistivity. The following expression relates these parameters to the apparent resistivity:

$$\rho_a = k\frac{\Delta V}{I} \tag{2.7}$$

When the measurement is made over a homogeneous surface, the apparent resistivity is equal to the true resistivity of the ground. However, when the resistance is measured over a complicated subsurface structure, the apparent resistivity is a weighted average of the resistivity of the various rocks below the surface.

2.1.5 Electrode configuration and array types

The different dispositions of the four-electrode system give rise to what are known as electrode arrays or configurations. Many electrode configurations are commonly used for ground-surface surveys. The most common of these being the Schlumberger, Wenner and the Dipole-dipole arrays, where the electrode separations relate to the investigation depth and lateral resolution, according to the sensitivity distribution of each arrangement.

There are even varied and numerous electrical prospecting arrays depending on number of electrodes and their distribution on the ground. The most appropriate survey configuration (vertical electrical sounding, profiling, electrical resistivity tomography ERT) will strongly depend on the specific objectives of the survey.

In order to investigate the ground structure and determine the individual formation resistivity, a series of measurements must be made with the electrodes in different positions. Three survey techniques have been developed for different applications.

1. Profiling (Constant Separation Traversing):-in these, the electrode spacing is kept constant and all the electrodes are moved laterally between measurements is used to examine lateral changes in the geological structure. Vertical and nearly vertical contacts between lithologic units are better mapped with this technique. These traversing techniques are popular, among others, in archaeological surveys but have largely been superseded by electromagnetic traversing methods for deeper investigations.

2. Vertical Electrical Sounding (VES, electrical depth probing or electrical drilling):- is a technique used to examine the vertical change in resistivity. In this technique, the spacing between electrodes is progressively increased between measurements, while the centre of the whole array is kept constant. As the electrode spacing increases, the current penetrates to greater depths and so a plot of apparent resistivity against electrode spacing provides a picture of the variation of resistivity with depth. In this case the data may be interpreted quantitatively to provide resistivity and thicknesses of subsurface layers.

3. **Electrical Imaging:-** this is a recent development which involves a combination of both traversing and sounding to produce an image along a section through the subsurface. The method is the focus of this thesis and detail discussion will be forwarded in the next section.

2.1.6 Electrical Resistivity Tomography (2D Imaging)

Conventional DC resistivity sounding and profiling has successfully capitalized on this aspect of resistivity surveying but is weak in respect of spatial coverage. By utilizing microcomputer control, the multielectrode resistivity method has overcome this weakness in resistivity surveying.

Two-dimensional (2D) geoelectrical resistivity imaging can be achieved by integrating the techniques of vertical electrical sounding with that of electrical profiling. It involves apparent resistivity measurements from electrodes placed along a line using a range of different electrode separations and midpoints. The procedure is repeated for as many combinations of current and potential electrode positions as defined by the survey configuration. 2D resistivity imaging can be seen as continuous vertical electrical sounding (CVES) in which a number of VES conducted in a grid are merged together or as a combination of successive profiles with increasing electrode spacing.

The direct current resistivity (DC) method has long been used for both mineral and groundwater exploration and various other engineering applications. Development of a multielectrode resistivity measurement system expanded the use of this method for engineering and environmental applications.

2.1.6.1 Field survey method and measurement procedure

Developments in the recent years have led the use of 2-D electrical imaging/tomography surveys to map areas with moderately complex geology (Griffiths and Barker 1993).

Nowadays, in many geophysical problems, the DC method is applied to detect target location, size and depth before excavation. In such an application, DC data are generally collected by a multi-electrode resistivity system as a sounding-profiling data along several parallel lines. These sounding-profiling data are inverted using a 2D resistivity inversion algorithm, and the resulting estimated 2D models are combined to create pseudo-three-dimensional resistivity images.

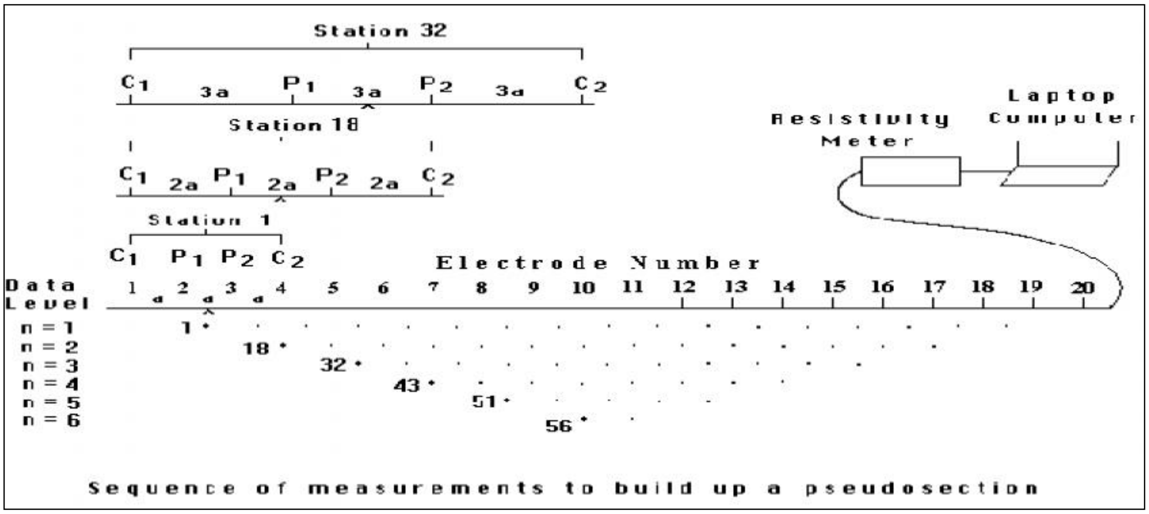

Figure 2.4 Measurement distribution of a surface resistivity arrangement that is used to build the resistivity pseudosection.

Measured data are presented as a pseudo-section in which the apparent resistivity is assigned to the midpoint of the four electrodes for each survey level (related to the spacing between current and potential electrodes). The pseudosection provides a smooth image of the 'true' resistivity structure with depth, so does not reproduce correctly either the electrical resistivity contrast between structures, or its exact spatial position. Solving the inverse problem is necessary to obtain the estimated resistivity with depth.

2.1.6.2 Electrode configuration of 2D imaging

There are different electrode arrangements with different applications used in electrical resistivity imaging survey. The most commonly known are Wenner (α, β and γ), Dipole-Dipole, Pole-Dipole, pole-pole and Wenner-Schlumberger arrays. The basic resistivity measuring technique is just similar to the conventional principles. Basically, four electrodes are required; two for current injection and two electrodes for potential measurement. Each array has their own advantages and drawbacks in data acquisition and processing works. But one might has better sensitivity and resolution power for vertical as well as lateral structural variations than the other. For instance, Wenner array in multi-electrode mode has good resolution power for horizontal structure having vertical variations but weak for horizontally variable geological structures.

Note that as the electrode spacing increases, the number of measurements decreases. The type of array used also matters the number of measurements to be obtained. The Wenner array gives the smallest number of possible measurements compared to the other common arrays used in 2-D surveys. The survey procedures followed in the pole-pole array are similar to that used for the Wenner array, whereas, survey procedures of dipole-dipole, Wenner-Schlumberger and pole-dipole arrays are slightly different. Wenner-Schlumberger array which is the emphasis of this paper will be discussed more.

Wenner-Schlumberger array

Among the multi-electrodes arrays, the Wenner-Schlumberger array has better resolution and high sensitivity for vertical and horizontal geological variations. The Wenner-Schlumberger array is a technique where different combinations of an electrode spacing 'a' and a factor 'n' can be used. The factor 'n' is the ratio of the distance between the C_1-P_1 (or P_2-C_2) electrodes to the spacing between the P_1-P_2 potential pair. It has value 1 for the first sequence of measurement and 2 for the next, and so on.

Wenner-Schlumberger is a recent hybrid from the Wenner and Schlumberger arrays for better 2-D imaging survey. The conventional Schlumberger array is one of the most commonly used array for resistivity sounding surveys. On the other hand, Wenner array is the successful procedure for profiling survey. The spacing between adjacent electrodes is 'a'. The first sequence of measurements is carried out, this array, with electrode spacing of '1a'. In this sequence of measurement, the first measurement is made with electrodes 1, 2, 3 and 4. In this case, electrodes 1 and 4 are used as the current electrode C_1 and C_2 respectively, and electrode 2 and 3 act as the potential electrode P_1 and P_2 respectively. For the second measurement, electrodes number 2, 3, 4 and 5 are used for C_1, P_1, P_2 and C_2 respectively. This is repeated down the line of electrodes until the last set of electrodes, 69, 70, 71 and 72, are used for the last measurement with '1a' spacing. For instance, a system of measurement with 72 electrodes will have $(72-3)=69$ possible measurements with '1a' spacing. This configuration has just the classical Wenner array.

The next sequence of measurements is made by choosing spacing a current electrode and a potential electrode to be ‘2a’ and the spacing between two potential electrodes is set to be ‘a’ (may be a fractional number) to get Schlumberger depth of investigation. In this case ‘n’ factor have a value 2.

First measurement is made using electrodes 1, 3, 4 and 6, and then the second measurement uses electrodes 2, 4, 5 and 7 for C_1, P_1, P_2 and C_2 respectively for each. But normally only one either of the two trends is taken. This process is repeated down the line until electrodes 67, 69, 70 and 72 are used for the last measurement with spacing ‘2a’. The same process is repeated for measurements with ‘3a’, ‘4a’, ‘5a’, ‘6a’andsoon. To understand more, a good figurative illustration of Wenner-Schlumberger electrode configuration is presented in the Figure 2.9 below.

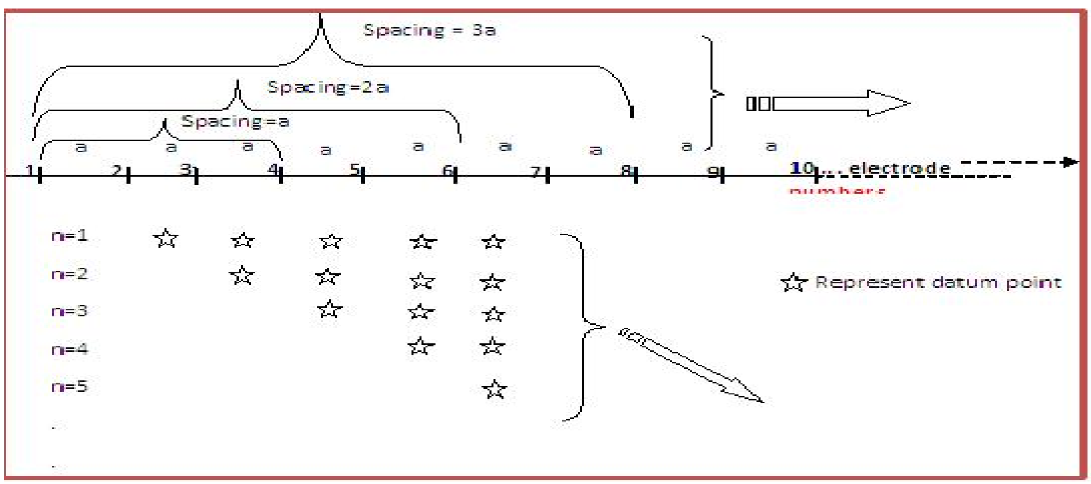

Figure 2.5. The Wenner-Schlumberger 2-D imaging array procedure.

Wenner-Schlumberger array is quite sensitive to both horizontal and vertical structures and is better applicable for areas where both types of geological structures are expected. The signal strength for this array is smaller than that for the Wenner array, but it is higher than the dipole-dipole array. The median depth of investigation (z) for the Wenner–Schlumberger array is moderately deeper than the dipole-dipole and Wenner arrays (Loke, 2000).

2.2 The Magnetic method

2.2.1 Introduction

Compasses and dip needles were used in the middle ages to find magnetite ores in Sweden, indicating the magnetic surveying technique as the oldest of all applied geophysical techniques. It is still one of the most widely used classical prospecting methods.

Magnetic method is a commonly used geophysical technique to identify and image subsurface targets in a wide range of applications from archeological site investigations to regional scale studies (Telford et al., 1990). It involves measurements of the direction, gradient, or intensity of the Earth's magnetic field caused by local differences in the magnetization of the subsurface rocks and soils and interpretation of variations in these quantities over the area of investigation. Magnetic surveys can be made on the land surface, from an aircraft, or from a ship. Most exploration surveys made today measure either the relative or absolute intensity of the total field or the vertical component. Measurements of magnetic intensity can be made with simple mechanical balances or with elaborate electronic instruments.

With the development in instrumentation and interpretation techniques, the method has become even more popular during the last 30 years. Many projects have been made for reconfirmation of prospective geothermal areas, analysis of regional relationships among known geothermal areas, and discovery of new geothermal prospects using the creation of a Curie point depth map as an integral part of the exploration.

Magnetic field strengths are now usually measured in *NanoTesla* (nT). The pre-SI unit, the gamma, originally defined as 10^{-5} Gauss but numerically equal to the nT, is still often used.

2.2.2 Basic principles

Everywhere on the Earth there is a natural magnetic field which moves a horizontally free-moving magnetic needle (magnetic compass) to magnetic north. The magnetic field is a vector field, i.e., it is described by its magnitude and direction.

The Earth's large-scale magnetic field is superimposed by small-scale magnetic anomalies related with magnetized rocks (Figure 2.6). Magnetization is a vector quantity which, simply speaking, is related with the concept of north and South Pole of a magnet. The vector of magnetization may have arbitrary orientation in a rock, and that is why geometrically identical causative bodies can show quite different magnetic anomalies. There are two situations to be taken into account: the location and orientation of a causative body in various latitudes, and the remanent magnetization.

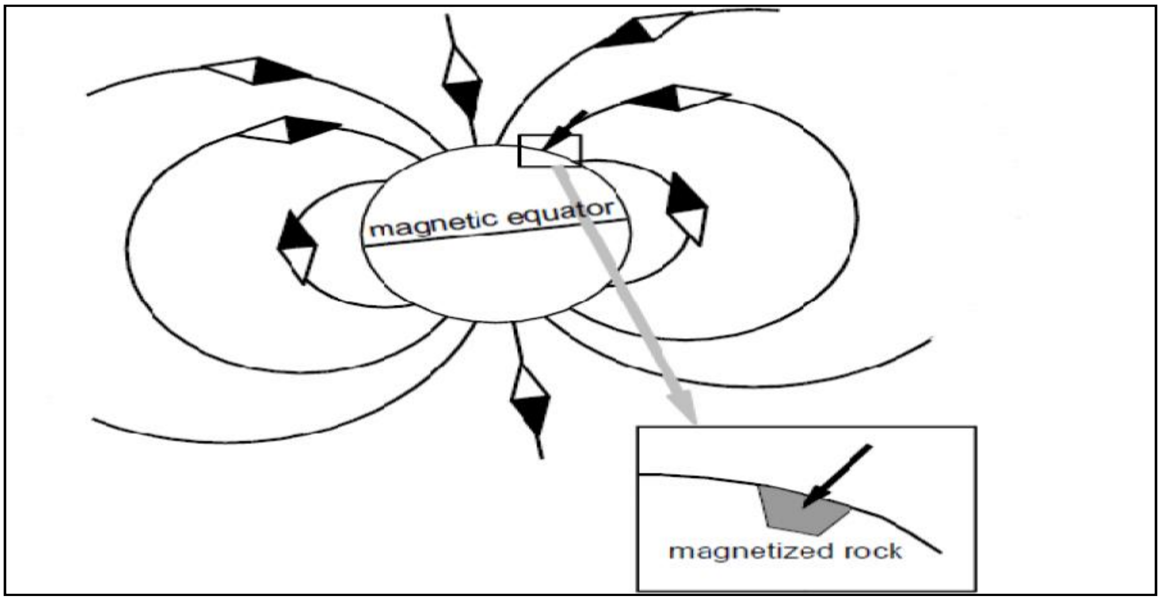

Figure 2.6 The Earth's magnetic field and the magnetization of rocks.

The magnetic method utilizes the variation in the strength of the Earth's magnetic field that reflects the spatial distribution of magnetized material throughout the subsurface. Magnetization occurs naturally in materials and rocks, and depends on the quantity of the magnetic minerals and on the strength and direction of the permanent magnetization carried by these minerals (magnetite, pyrrhotite). Although magnetic data do not respond directly to the presence of water, they can contribute to the understanding of the geologic controls on the groundwater systems. Magnetic surveys can be useful in hydrogeological studies due to their ability to determine basin geometry, to delineate igneous intrusions that my affect groundwater flow, and to identify shallow local magnetic anomalies caused by faults, paleochannels, eolian deposits or man-made features, intrasedimentary faults, and hence the compartmentation or connection within the aquifer system (Grauch et.al, 2001).

2.2.2.1 Magnetizing force, Laplace's equation and magnetic field

The magnetizing force (intensity of the magnetizing field) H at any point in space, where there is no electric current and, therefore no magnetic mass, as the gradient of magnetic potential W can be expressed as:

$$H = -\text{grad}W \tag{2.8}$$

where **W** is a function of position satisfying Laplace's equation. i.e.

$$\nabla^2 W = \frac{\partial^2 W}{\partial x^2} + \frac{\partial^2 W}{\partial y^2} + \frac{\partial^2 W}{\partial z^2} = 0 \tag{2.9}$$

(where x, y, z are Cartesian orthogonal co-ordinates).

2.2.2.2 Forces associated with magnetic poles

Charles Augustine de Coulomb, in 1785, showed that the force of attraction or repulsion between electrically charged bodies and between magnetic poles also obeys an inverse square law like that derived for gravity by Newton.

The mathematical expression for the magnetic force experienced between two magnetic monopoles is given by

$$F_m = \frac{1}{\mu}\frac{p_1 p_2}{r^2} \tag{2.10}$$

where **μ** is a constant of proportionality known as the **magnetic permeability**, P_1 and P_2 are the strengths of the two magnetic monopoles, and r is the distance between the two poles.

The constant **μ** depends upon the magnetic properties of the medium in which the poles are situated. This force is attractive, if the poles are different in sign, and repulsive if they are of the same sign.

2.2.3 Magnetic susceptibility

The intensity of magnetization, *I*, is related to the strength of the inducing magnetic field, *H*, through a constant of proportionality *k*, known as the magnetic susceptibility.

$$I = kH \tag{2.11}$$

Magnetic susceptibility is a non dimensional quantity that is determined by the physical properties of the magnetic material. It can take on either positive or negative values. Positive values imply that the induced magnetic field, *I*, is in the same direction as the inducing field, *H*. Negative values imply that the induced magnetic field is in the opposite direction as the inducing field.

The space in which magnetic forces act on a magnet or coil, through which a current is flowing, is called the magnetic field. The force associated with the magnetic field is characterized by the magnetic induction B (the magnetic field vector); which is given by

$$B = \mu H \tag{2.12}$$

where $\mu = \mu_r \mu_o$ the permeability of the medium, the product of relative permeability and permeability of free space.

Thus the above equation can be written as

$$B = \mu_o (1 + k) H \tag{2.13}$$

Rearranging to introduce $k = \mu_r - 1$ and we have

$$B = \mu o H + \mu o k H = \mu o (H + I) \tag{2.14}$$

In magnetic prospecting, the susceptibility is the fundamental material property whose spatial distribution we are attempting to determine. In this sense, magnetic susceptibility is analogous to density in gravity surveying.

Table 3 Ranges of values for the magnetic susceptibility K of different rocks, compiled by Schön (1983) (after Knodel et al, 2007)

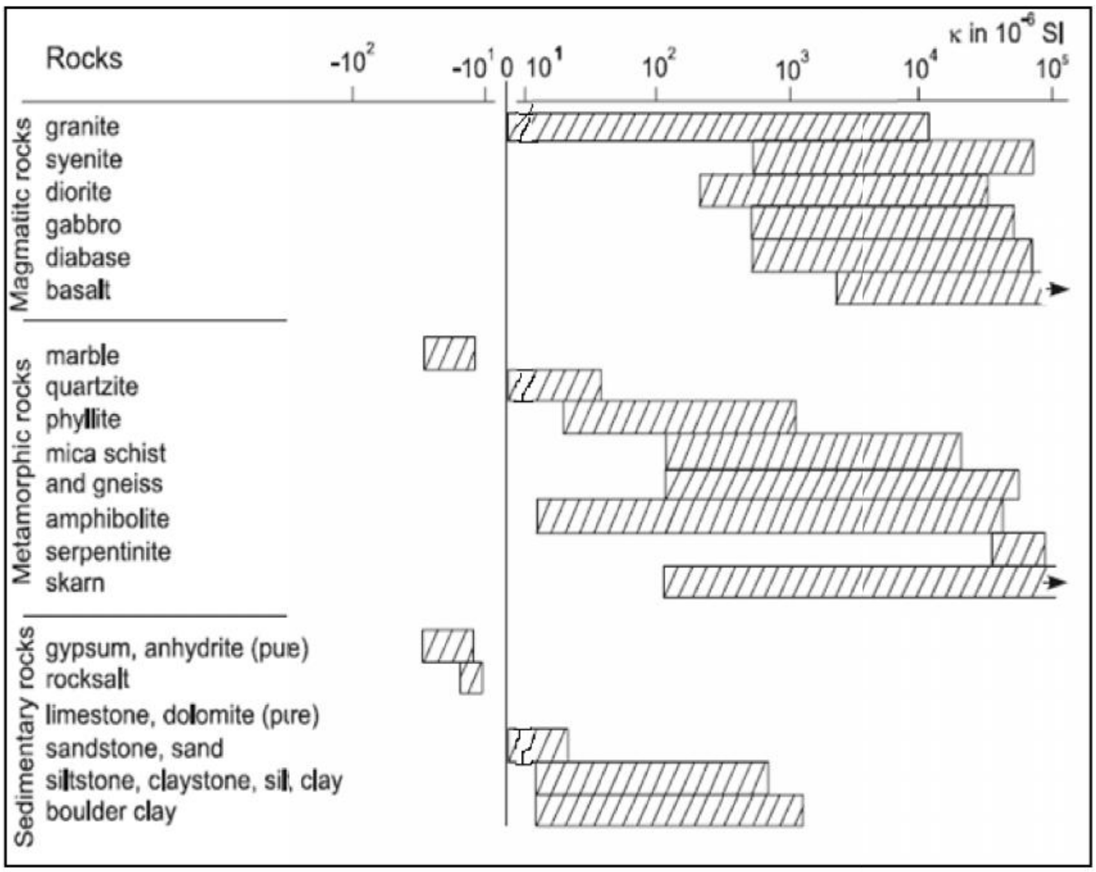

2.2.4 The Earth's Magnetic Field

The Earth's magnetic field consists of three components: 1) the main field, 2) the external field (fluctuating field) and 3) magnetizable materials within the Earth's crust (local anomaly field).

The main field which accounts for over 99% of the earth's total magnetic field is internal in origin and is thought to be caused by convection currents of conducting material (mainly iron and nickel) within the liquid outer core. The earth's main magnetic field approximates to a first degree a magnetic dipole and is the inducing field for magnetizable objects within the earth's crust. The main field consists of several magnetic elements, which are important in understanding the measured magnetic anomaly patterns. These elements include: 1) magnitude of the field (F), 2) magnetic inclination (I) which is the dip of a magnetic compass needle from horizontal (e.g., magnetic south pole is -90^{o} , magnetic north pole is 90^{o}, and magnetic equator is 0^{o}), and 3) magnetic declination (D) which is the angle between geographic and magnetic north. Figure 2.3 shows the relationship between these values and are collectively known as the International Geomagnetic Reference Field (IGRF).

Additionally, the Earth's main magnetic field changes with time due to variations in the motion of the convection currents within the outer core. These changes (called westward drift or secular variations) cause the magnitude, inclination and declination to change with time. As a consequence, the IGRF is updated every ten years or so and is revised to give the DGRF (Definitive), which is current reference model of the earth's magnetic field. The current DGRF can be obtained from the national geophysical data center of the National Oceanic and Atmospheric Agency (NOAA, 2011).

The external magnetic field (also called diurnal variations) is due to electric currents within the earth's ionosphere. These currents are mainly caused by interactions with plasmas connected with solar winds. These diurnal variations fluctuate rapidly but smoothly with time (minutes to hours) with maximum amplitudes varying from 50 to 200 gammas. On some days, these fluctuations are more random with amplitudes of several hundred gammas and are called magnetic storms. These storms are associated with solar flares and sunspot activity, and may persist for hours or several days. During such storms, magnetic surveying should be stopped.

The magnetizable materials within the earth's crust create small amplitude magnetic fields that cause spatial variations of the earth's main magnetic field. These materials are the targets of the magnetic method.

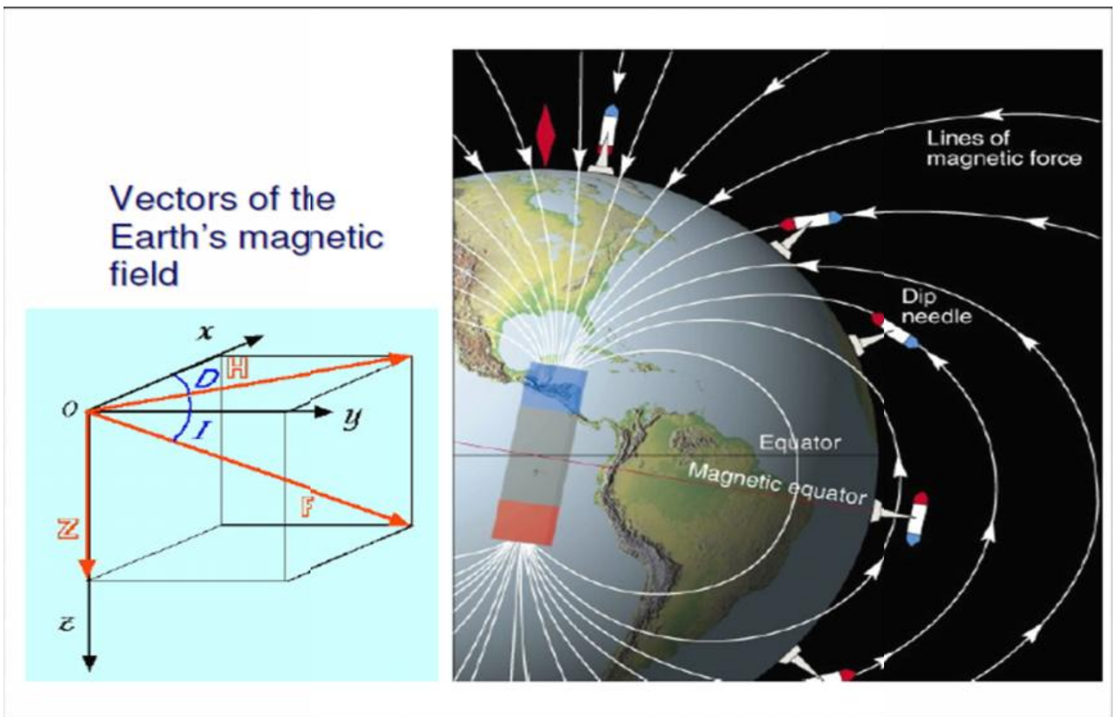

Figure 2.7 Elements of the Earth's magnetic field.

2.2.5 Magnetic Properties of rocks

The magnetic readings measured by a magnetometer are usually assumed to be caused by magnetization induced in a magnetizable material (those with a large magnetic susceptibility) by the earth's main magnetic field. This magnetization is not permanent and is lost when the external field is removed. In addition, most rocks and minerals have a permanent magnetization called remnant magnetization that is acquired by a variety of mechanisms (Telford et al., 1990) and is usually in a different direction and magnitude than the induced magnetization. In most cases, the magnitude of the remnant magnetization is small compared to the induced magnetization and can be ignored, although for detailed surveys (source anomalies less than 5 gammas) it can be important, requiring laboratory analyzes to determine the remnant magnetization properties of the rock or soil samples. All matter responds to an applied magnetic field, due to the effect of the field on electron motions in atoms, although the response is very weak for most materials. There are three types of magnetic materials: paramagnetic, diamagnetic, and ferromagnetic.

Diamagnetism this is a special case of paramagnetism in which there is an almost perfect alignment of electron spin directions within large portions of the material referred to as ***domains***. Like paramagnetism, ferromagnetism is observed only at temperatures below the Curie temperature. There are three varieties of ferromagnetism.

As is known, crustal rocks lose their magnetization at the Curie point temperature. At this temperature, ferromagnetic rocks become paramagnetic, and their ability to generate detectable magnetic anomalies disappears. The Curie temperature for titanomagnetite, the most common magnetic mineral in igneous rocks, is less than approximately 570°C. It has been established that an increase in titanium content of titanomagnetite causes a reduction in Curie temperature and the titanium content generally increases in the more mafic igneous rocks (Byerly and Stolt, 1977). Consequently, it may be possible to locate a point on the isothermal surface by determining the depth to the bottom of a polarized rock mass. Thus the deepest level in the crust containing materials which create discernible signatures in a magnetic anomaly map is generally interpreted as the depth to the Curie isotherm.

One of the important parameters which determine the relative depth of the isotherm with respect to sea level is the heat content in a particular region. The heat content is generally proportional to the local temperature gradient, thermal capacity, and generation of heat. A region with significant geothermal energy near the surface of the earth is characterized by an anomalously high temperature gradient and heat flow. It is therefore to be expected that regardless of the composition of the rocks, the region will be associated with a conspicuously shallow Curie point isotherm relating to the adjoining regions isotherm (Bhattacharyya and Leu, 1977).

2.2.6 Noise and Corrections for Magnetic Variations

All magnetic data sets contain elements of noise and will require some form of correction to the raw data to remove all contributions to the observed magnetic field other than those caused by sub-surface magnetic sources. In ground magnetometer surveys, it is always advisable to keep any magnetic objects (keys, penknives, some wristwatches, etc), which may cause magnetic noise, away from the sensor. It is also essential to keep the sensor away from obviously magnetic objects such as cars, metal sheds, power lines, metal pipes, electrified railway lines, walls made of maffic rocks, etc.

There are several ways of correcting magnetic data according to the various magnetic variations. For the secular variation of magnetic data a model is known as International Geomagnetic Reference Field (IGRF) has been prepared from comparison of individual magnetic responses in different areas of magnetic observatories. So, it has become standard processing practice for magnetic survey that the applicable IGRF (updated to the time of the survey) is subtracted from the observed values of the total magnetic intensity.

The most significant correction is for the diurnal variation in the Earth's magnetic field. The necessary corrections are mostly attempted by the reoccupation of the base station which is located in or near the survey area.

Variations in magnetic field due to magnetic storms can be so rapid, unpredictable, and of such large amplitude, that normally no corrections can be made. Magnetic surveying is therefore generally discontinued under these conditions.

CHAPTER THREE

DATA ACQUISITION AND PROCESSING

3.1 2D Resistivity Imaging

Multi-electrode (usually 72-electrode or 48-electrode), micro-processor based 2-D Resistivity Imaging System offers good opportunity to obtain the resistivity images to reasonable depths around 50-100 m (much depends on local geological conditions) below the surface level. For a good lateral and vertical resolution the hybrid Wenner-Schlumberger profiling is preferred.

The multi-electrode Resistivity Imaging System, IRIS made SYSCAL Pro $R1^+$ Switch 72, was used in the study region. A *GARMIN* GPS was used for the location of the position of the electrodes and this data was used for the topographic correction for all the profiles in the RES2DINV program (Figure3.2).

The electrical tomography surveys at Gergedi thermal springs were conducted on three lines (Figure 3.3) with inter electrode spacing of 5 m, thus utilizing the available whole cable length of the instrument at our disposal. For each profile, more than 1000 measurements (data points) were acquired using main and roll along sequences. The imaging lines were appropriately selected to cross potentially interesting thermal zones and specifically **Line-1** was selected to straddle the currently active thermal centers while **Line-2** runs parallel to **Line-1** and about 400 m north of it and crossing the two small streams that drain the springs to the Awash River. **Line- 3** also runs almost parallel to the first two lines but lies across and on the northern side of Awash River. The beginning and end coordinates of these three lines are given in the Table below (Table 4).

ELECTRE II software permits to load a preset sequence of measurement (Schlumberger-Wenner, in this case) into the internal memory of the resistivity meter. This program displays the theoretical depth of penetration reached by the sequence (65m in this case).The acquired data is transferred from the SYSCAL Unit to a PC by the PROSYS software and using this same software data from rollalong sequences were added to the main sequence data. As a first stage of interpretation of the data, an automatic filtering exercise was performed for the elimination of noise from again with the PROSYS software. Topography data were also inserted and the apparent resistivity values recalculated, before exporting the data for further processing with the inversion software.

Table 4. GPS location of the beginning and end coordinates of imaging lines.

Traverse	**Main + Roll along sequences UTM Coordinates (m)**						**Remark**
	Beginning of Line			**End of Line**			**(traverse orientation)**
	Easting	**Northing**	**Elev. (m)**	**Easting**	**Northing**	**Elev.(m)**	
Line-1	521428	935083	1552	521010	935001	**1562**	Line passing over and south of the thermal manifestation areas
Line-2	521684	935218	1564	521070	935353	1557	Traverse line about 400 m north of Line-1 and crossing the streams draining to River Awash
Line-3	522217	936032	1551	521434	936106	1555	On the north side and across the Awash River and running almost parallel to it

After performing all necessary correction and filtering under PROSYS software environment, as outlined above, the data were exported to **RES2DINV** Inversion software to create 2D inverted model section. This resistivity inversion software is based on the least-square method proposed by Loke and Barker (1996).

The program **RES2DINV** automatically subdivides the subsurface into a number of blocks and then uses a least-square inversion scheme to determine the appropriate resistivity values for each blocks so that the calculated apparent resistivity values agrees with the measured apparent resistivity values from the field survey. The results are displayed as inverted model resistivity sections versus depth of the subsurface along the profile. Figure (3.1) shows the measured apparent resistivity pseudo section (A), and calculated apparent resistivity pseudo section (B) and Figure (3.2) shows inverted model resistivity section with topography.

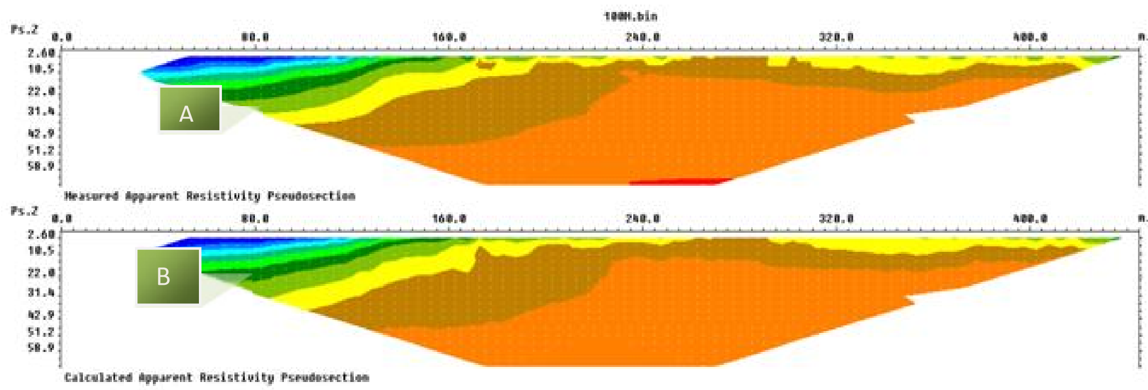

Figure 3.1 measured (A) and calculated (B) apparent resistivity pseudo sections

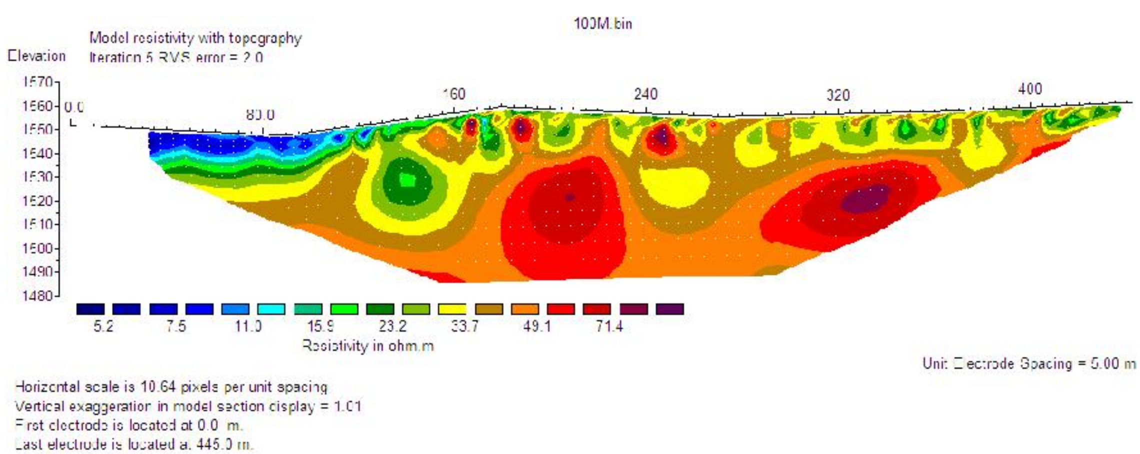

Figure 3.2 inverted model resistivity section with topography

The inverted resistivity data were also exported in surfer format and after gridding, the same sections were plotted using surfer. Inverted resistivity sliced depth section for different depth were also prepared from the data after it is exported in to surfer.

3.2 Magnetic Survey

Ground based magnetic measurements were done, with GPS survey, using portable instruments of Scinterx made Proton Precision Magnetometer MP-2 working in total field mode, at regular intervals of 40-50m over the survey area. The GPS data is used to locate the position of the magnetic stations and to correct the magnetic data for the IGRF.

Magnetic data were collected on grids, two base stations were established, due to River Awash crossing the survey area, a single base station were impossible, for the diurnal correction of magnetic data and over 500 magnetic data were collected in the survey area. At each station the magnetometer reading, recording time, its location in UTM coordinate were recorded and a tuning field of 35,500 nT was selected for the magnetometer reading.

The observed magnetic field data were corrected for diurnal variation using the base station reading taken at the beginning and reoccupation reading after each hour survey. The main magnetic field at the survey area is obtained from international geomagnetic reference field (IGRF) and it is subtracted from diurnal corrected total field, then the anomalous field values are gridded using surfer 9 (Golden Software, 2010) and Oasis Montaj software (Geosoft ,2004).

In addition to the total magnetic intensity map, data enhancement techniques were applied to produce other maps, which may help to recognize more features. These are done by using the Geosoft software package called Oasis Montaj.

Due to the dipolar nature of the geomagnetic field, magnetic anomalies observed anywhere rather than magnetic poles are asymmetric even when the causative body distribution is symmetric. This property complicates the interpretation of magnetic data. Reduction to the pole (RTP) is a technique that converts magnetic anomaly to symmetrical pattern which would have been observed with vertical magnetization. This technique usually is applied in frequency domain which has some disadvantages such as noise induction, necessity of using fixed inclination and declination throughout survey area, its unstability in low magnetic latitude and also unknown remanent magnetization that in many cases restrict its applicability (Ansari and Alamdar, 2009).

Analytic signal is a suitable quantity that can be calculated either in space or frequency domain and its amplitude is independent to magnetization direction. In this paper, analytic signal has been used as RTP operator and applied on the magnetic data from an area at the Gergedi thermal springs.

The upward continuation is also applied on the magnetic data. Near surface (high frequency) features are attenuated as the magnetic data virtually moves upward (Sheriff, 1989). On a higher surface, the regional patterns tend to be displayed more clearly, and local anomalies become less evident.The magnetic data (residual anomaly and amplitude of analytical signal) also presented in cross sections along the three imaging lines to compare with the resistivity sections.

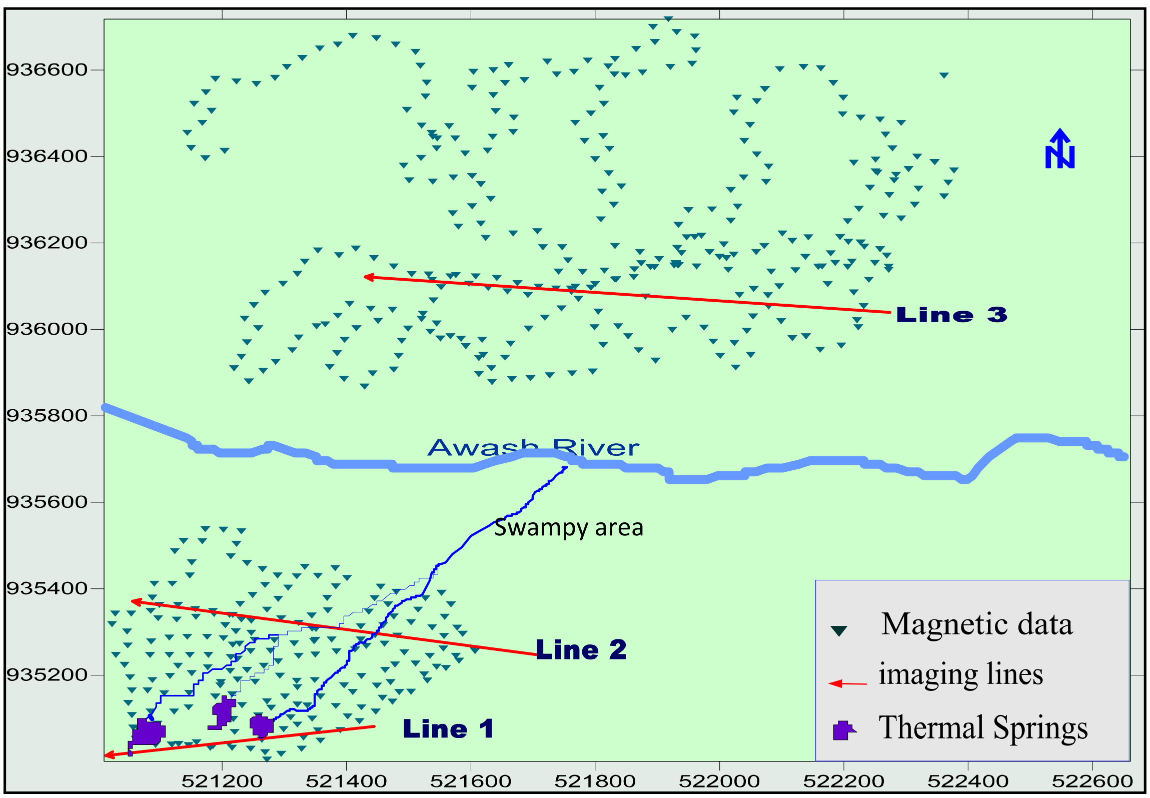

Figure 3.3 Magnetic data distribution, imaging lines and location of active thermal springs over Gergedi Area

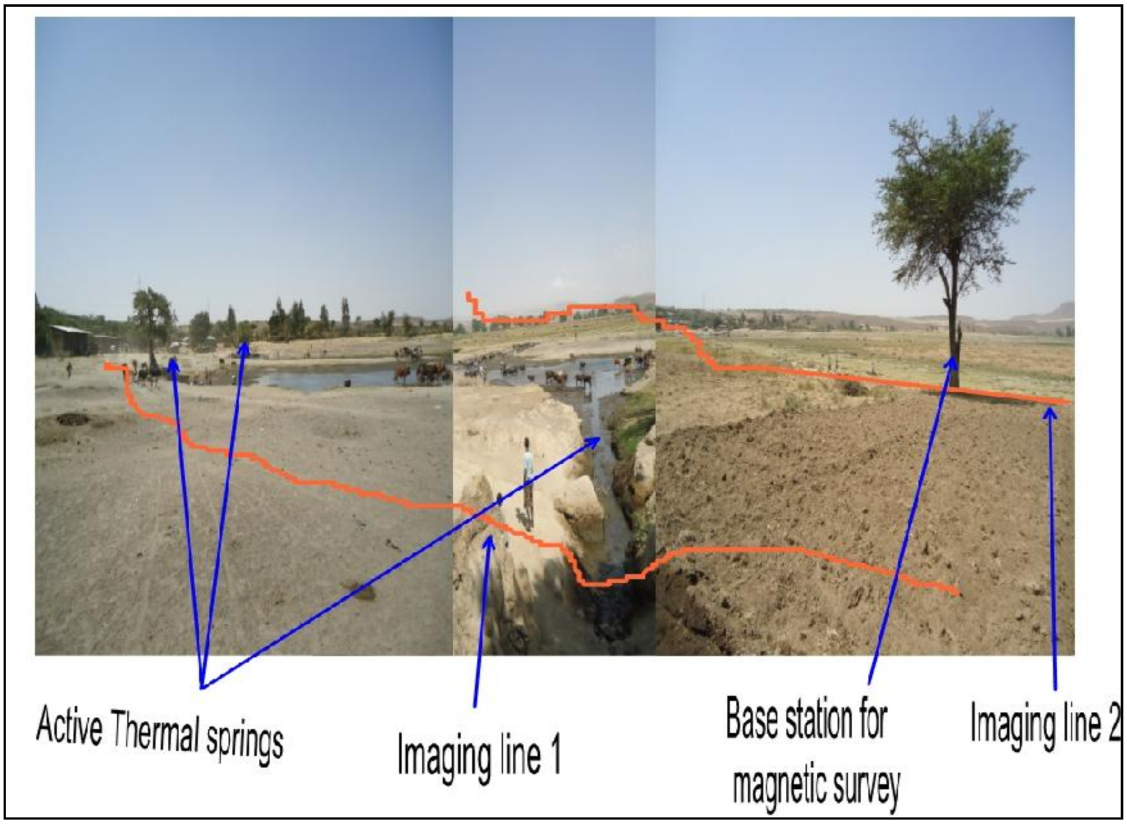

Figure 3.4 Field Photographs showing imaging traverses of Line 1 and 2; active thermal springs and base station for magnetic data.

Figures (3.3 and 3.4) show distribution of magnetic data and resistivity imaging traverses with the active thermal springs. Those springs are currently underused for healing purposes. Figure (3.2) is the photograph indicating the active thermal springs and the first 2 imaging traverses over the springs and the first base station for magnetic survey also indicated.

CHAPTER FOUR

RESULTS, INTERPRETATION AND DISCUSSION

Geophysical data is presented and interpreted in a variety of forms, depending upon the method used and the objective of the survey that we need to achieve. The outputs of these geophysical data were used to produce different anomalies which show contrast in the physical quantity of the subsurface materials. In this study 2D electrical resistivity sections and resistivity stacked plot maps from the electrical imaging data, and from the magnetic data residual magnetic anomaly and analytical signal maps of the area and magnetic profile plots corresponding to the resistivity lines, and upward continued magnetic maps were prepared and presented. The interpretation of these maps and profiles are forwarded.

4.1 RESISTIVITY DATA

4.1.1 INTRODUCTION

Resistivity is a fundamental electrical property of rocks, which is closely related to rock lithology of which the main controlling factors are effective rock porosity, pore structure, amount and salinity of pore-filling fluid, temperature and the presence of clays. The effect of clay over the resistivity is important in geothermal areas since clayey alteration minerals are very frequent, particularly in volcanic rocks.

To convert the resistivity picture into geology, some knowledge of the typical resistivity values for the different types of subsurface materials and geology of the survey area is required. Thus in this discussion on interpreting electrical data, the geological knowledge of the study area from previous different studies and resistivity ranges of different rocks are used for the interpretation of the inverted 2D electrical imaging sections.

In the following, inverted 2D resistivity sections for Lines 1, 2 and 3 with corresponding residual magnetic anomaly and analytical signal profiles extracted from the gridded anomaly map of magnetic data of the survey area are presented and stacked plots of inverted resistivity sections for different depths are prepared and discussions are forwarded.

4.1.2 PROFILE LINE 1

Survey Line-1 has a total length of 450 m and, as indicated in the discussion of the previous chapter, it has NE to SW orientation straddling the active thermal springs at Gergedi. An interpreted 2D inverse resistivity model section for this line is given in Figure 4.1. A total of1121 data points were used for the inversion and has produced resistivity ranges of 4.3-78.4 Ohm-m with optimum depths of around 68 m. The aim of the survey was to map the presence of fractures (weak zones) that could potentially act as conduits for the thermal springs and to infer where the water comes from and also to map the zones within the area that are affected by thermal alterations. As in the previous studies the possible water recharging sources are expressed as Lake Koka (Tigistu Haile and Tamiru Alemayehu, 2010; Theodrose Solomon, 2008).

It is clear from the figure that the subsurface shows regions of low resistivity zones at shallow depth followed by regions of relatively medium and higher resistivity at depth. The section can be separated as layers and are interpreted as the first layer of 3-20 Ohm-m resistivity representing the response of the top soil cover with higher salinity due successive capillary rise of fluids and subsequent evaporation. This layer extends to a depth of 20m at the first electrodes (at 0m on the surface, where the measurement of imaging line starts) and fades out around 160m along the survey line towards SW. The low resistivity of this layer is due to the salinity and high moisture content of the soil, this condition is justified by surface manifestations and its average thickness is determined as 10m.

The second layer with resistivity ranges of 25-50 Ohm-m also has an average thickness of 10m and depths varying between 30-40 m at the beginning of the line (0 m on the surface) and extends to depths of 65 m between horizontal distances of 100m and 300m (on the middle of the section).This horizon could be geologically interpreted as fractured basalts and it is very likely representing the zone of thermal fluid rise. As one can see from the inverted model section, the layer is totally weathered at the most northeastern end of the section and it is highly thermally altered towards the southwest.

The third layer has resistivity ranges of 50-80Ohm-m, relatively higher resistivity; it starts from depths of 35m to 65 m (maximum depth of this section). At distances of 150, 250 and around 350 m the layer shows discontinuities along the profile and the layer is highly affected by alteration as a result of the thermal fluids, these discontinuities could be interpreted as faults. This result is also supported by the magnetic profiles. The springs (the three Gergedi thermal springs) are clustered between distances of 125m and 350m; these indicated faults could be the passageway of thermal water for the springs. From geological successions given in different studies (Alula et.al, 1992, Tigistu Haile and Tamiru Alemayehu, 2010), reviewed in chapter one of geology section, the layer may constitute a weathered ignimbrite.

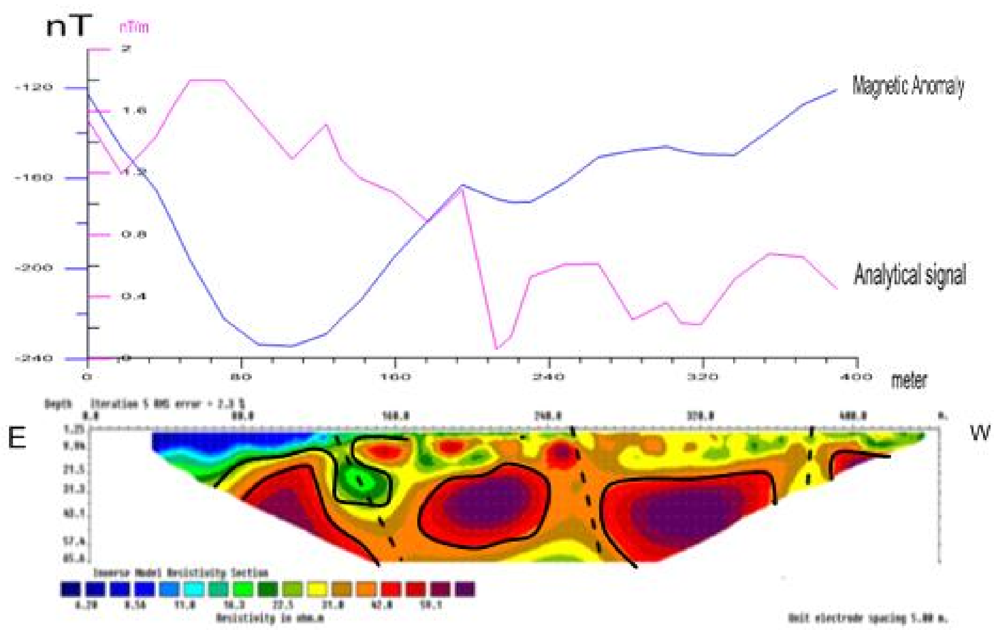

Figure 4.1 Inverted resistivity sections of Line 1 and residual magnetic anomaly and amplitude of analytical signal of the magnetic anomaly profiles along Line 1

The magnetic profile plot along this line (Line 1) shown on top part of Figure (4.1) shows variation of magnetic anomaly and amplitude of the analytic signal verses distance along the traverse. The residual magnetic signature obtained from the magnetic anomaly plot along this traverse shows considerable variation in amplitude from a minimum negative peak value of about -240nT at a distance of about 125 m from the initial station position and a maximum negative peak value of about -110nT at distances of about 0m and 400m (Figure 4.1).

As shown from the plot the negative anomaly starts decreasing from the beginning until it reaches 125m to its minimum negative value, then after, the amplitude is increasing except at indicated local minima at distances of around 250 and 350 m. These low magnetic anomaly responses (peaks) could be associated with the presence of weak (fractured) zones that could be interpreted as fault lines. These zones are clearly demarcated in the resistivity plot and are indicated in the section as doted lines.

The amplitude of the analytical signal (Nabiaghan, 1972; and Sundrarajan 1983), which insures precise location of structures and boundaries of the causative sources were also computed. With many other local minima and maxima the analytic signal plot is bounded by 0.16nT/m minimum and 1.81 nT/m maximum values. The prominent peaks found on the amplitude of the analytical signal (Figure 4.1) correspond to the contacts/faults also depicted on the electrical resistivity section. These features are also reflected from the residual magnetic anomaly profiles as discussed above.

4.1.3 PROFILE LINE 2

Figure (4.2) gives the geo electrical layering of the ground beneath profile Line 2 of the Gergedi thermal spring. It is seen from the figure that the subsurface is represented by different resistivity values ranging from 0-120 Ohm-m. This survey line crosses three small streams that merge a few tens of meters just north of the traverse.

As in the above section for Line 1, this true resistivity model section can be seen to exhibit three distinct resistivity zones, each segregate`d by a relatively flat boundary. In general, three zones are mapped:- the relatively low resistivity of (0-6 Ohm-m) top layer, the medium resistive layer of resistivity 6-25Ohm-m at intermediate depth and a resistive layer of resistivity 30-120 Ohm-m forming the bottom stratum mapped by the survey depth. The geological interpretation of the above layers are the top layer comprises of top soil cover of thickness of about 21 m, this layer as in above section (Line 1) is affected by salinity and is with high moisture content as a result of which it gives low resistivity response. Within this layer and at its bottom, at a distance of about 170 to 280 m along the traverse, is a very low resistivity zone possibly the direct effect of seeping water from the streams. The layer underlying this conductive top layer could be a weathered ignimbrite extending from a depth of about 21 to 31 m (10m thickness from the underlying layer) and is a highly thermally altered rhyolitic zone. The last layer mapped by the survey is relatively resistive and shows discontinuity along the profile.

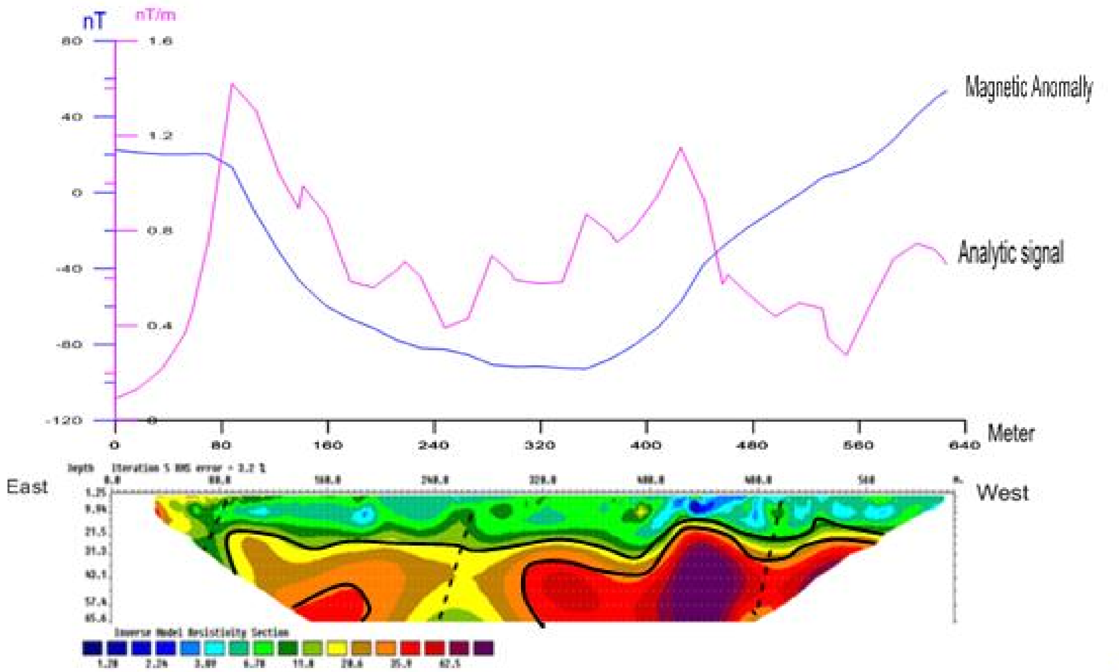

Figure 4.2.Inverted 2D resistivity sections of Line 2 and residual magnetic anomaly and amplitude of analytical signal plot along the line.

From the inverted sections, three zones of subsurface weakness are clearly apparent. Two regions of subsurface discontinuity extending to greater depth and located around 270 m and 510 m from the beginning of the survey line are indicated. These could be interpreted as weak/faulted zones through which fluid circulation from the surface and shallow depths are possible. These weak zones/fractures may act as the recharging path of water for the springs and the associated streams that discharge the thermal spring waters to River Awash.

The residual magnetic anomaly profile of the line, given in the top part of Figure 4.2 shows minimum and maximum residual magnetic anomaly values of -90 and 55 nT at 320m and 620m respectively. The profile shows a saddle at the middle of the traverse bounded by relatively high anomalies of 20 and 10nT indicated at distances of 80 and 520m respectively.

The profile also shows locally low anomalies that very well correspond with the weak zones in the depicted from the resistivity section.

The profile has low anomalies covering almost the entire surface of the middle section. This middle section shows relatively thick highly altered soil cover which has resulted in low magnetic response.

As shown in the section of Figure 4.2 the area is intensively fractured and this may be due to thermal alteration and since the study area is situated in the Ethiopian Rift with intense tectonic activity and high thermal water action these types of response are expected. The analytical signal plot over the section shows high and low values with major peaks over the faults supporting the responses in the resistivity section and residual magnetic plots over the profile.

4.1.4 PROFILE LINE 3

This is the third line over which electrical imaging surveys were done and the line runs almost parallel to Lines1 and 2 but is on the northern side of River Awash and constitutes the longest of the survey line among those conducted in the area. According to the results obtained through the inversion process, resistivity ranges of around 1-60 Ohm-m through penetrating depths of 66m were produced. In this profile 2027 data were measured on 805m long traverse- a traverse length which is covered with one main sequence and five rollalong sequences. The software (Res2Dinv) uses 14 layers and 1901 blocks to invert the resistivity data and cease with 4.58% of root mean square error and the model is accepted such that the RMS error shows no significant difference on the iteration process.

Figure 4.3 shows the 2D electrical imaging model section along this line (Line 3), a line which extends approximately east to west across the survey area and to the north of Awash River. The inverted 2D section for this line shows a relatively thin low resistivity top section as compared to those on Lines 1 and 2. In general, the section has overall resistivity ranges of 0.3-50 Ohm-m and is covered at the top almost entirely by low resistive materials, of which the region with resistivity values of 0.3-8Ohm-m is deduced as the soil cover with high salinity. This layer has on the average around 18m thickness. The next and 8-30 Ohm-m resistive material covers most part of the subsurface with discontinuities at distances of around 100,200 and 350 meters along the traverse from the eastern and beginning end of the line. These are deduced to be weak zones that possibly are the continuation of the faults/weak zones mapped on Line 1 and Line 2. Geologically, this layer may be interpreted as the highly weathered basalt.

Beneath this second layer is an extensive region of relatively high resistivity (30 –50 Ohm-m), again with discontinuous regions extending to depth at three locations. This layer is interpreted as the weathered ignimbrite and the variations in resistivity are the responses of various degrees of weathering and alteration of the rock units.

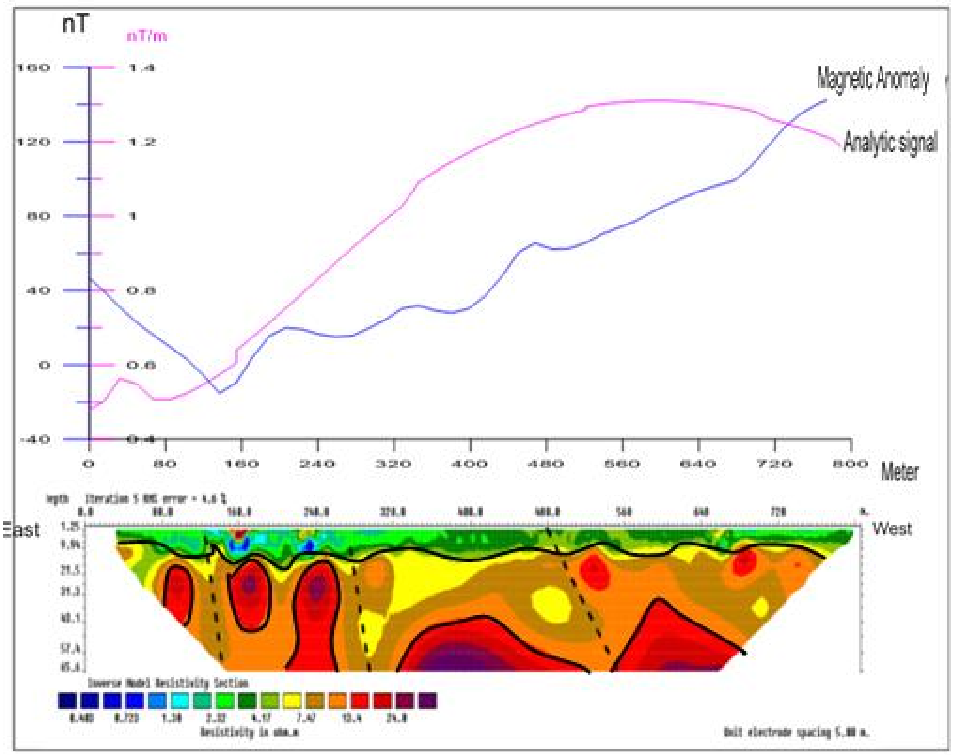

Figure 4.3 Inverted resistivity sections of Line 3 and residual and analytical signal magnetic profiles along the line.

The residual and analytic signal magnetic profile plots for this line are shown on the top part of Figure 4.3. Since variations in magnetic anomaly signature possibly indicate structurally controlled subsurface features (Adepelumi et.al., 2008, Telford et.al., 1990), it possible to interpret the profile plots with this perception. From the figure, it is seen that the residual magnetic plot shows minimum anomaly value of -10 nT at 130m and maximum magnetic anomaly values of 150nT at 800m. Generally the magnetic value increases to the west of the profile (section) except at the begging which shows a sharp decrease around 130m indicating existence of weak zones around this region. This fact is also indicated in the resistivity section. This signatures of this feature are also apparent on the analytic signal and their interpretation as a response of a subsurface discontinuity is in agreement with the above discussion. Other low magnetic responses are recorded throughout the length of the traverse showing insignificant contrast may be from shallow responses of the top soil but are indicated in the resistivity section as weak zones.

4.1.5 Stacked Maps of Resistivity Imaging

To determine the behavior of the overall resistivity variation of the survey area at different depths as well as horizontally, a stacked map of the resistivity imaging sections are prepared at different depths. The resistivity values and the depths are determined from the inversion process in Res2Dinvsoftware and exported to Surfer since the software has this option. Therefore, the parameters used to obtain these stacked plots are the inverted resistivity and depths.

Figure. 4.4 represent the variations of resistivity from shallower level (depth of 3m) down to deeper horizons (depth of 65m) as attained by the imaging survey.

This stacked plot (Figure 4.4), sketched using data of selected depths, shows the relative variation of the resistivity value of the whole area both laterally as well as vertically. As a general overview the area has low resistivity values with resistivity ranges of 0.3-120 Ohm-m. The maximum depth of penetration is 65m (maximum depth of penetration of multi electrode resistivity imaging with 5m electrode spacing is 65-100m, and for the Wenner-Schlumberger imaging sequence employed in this work, this results in the depth of 65 m).

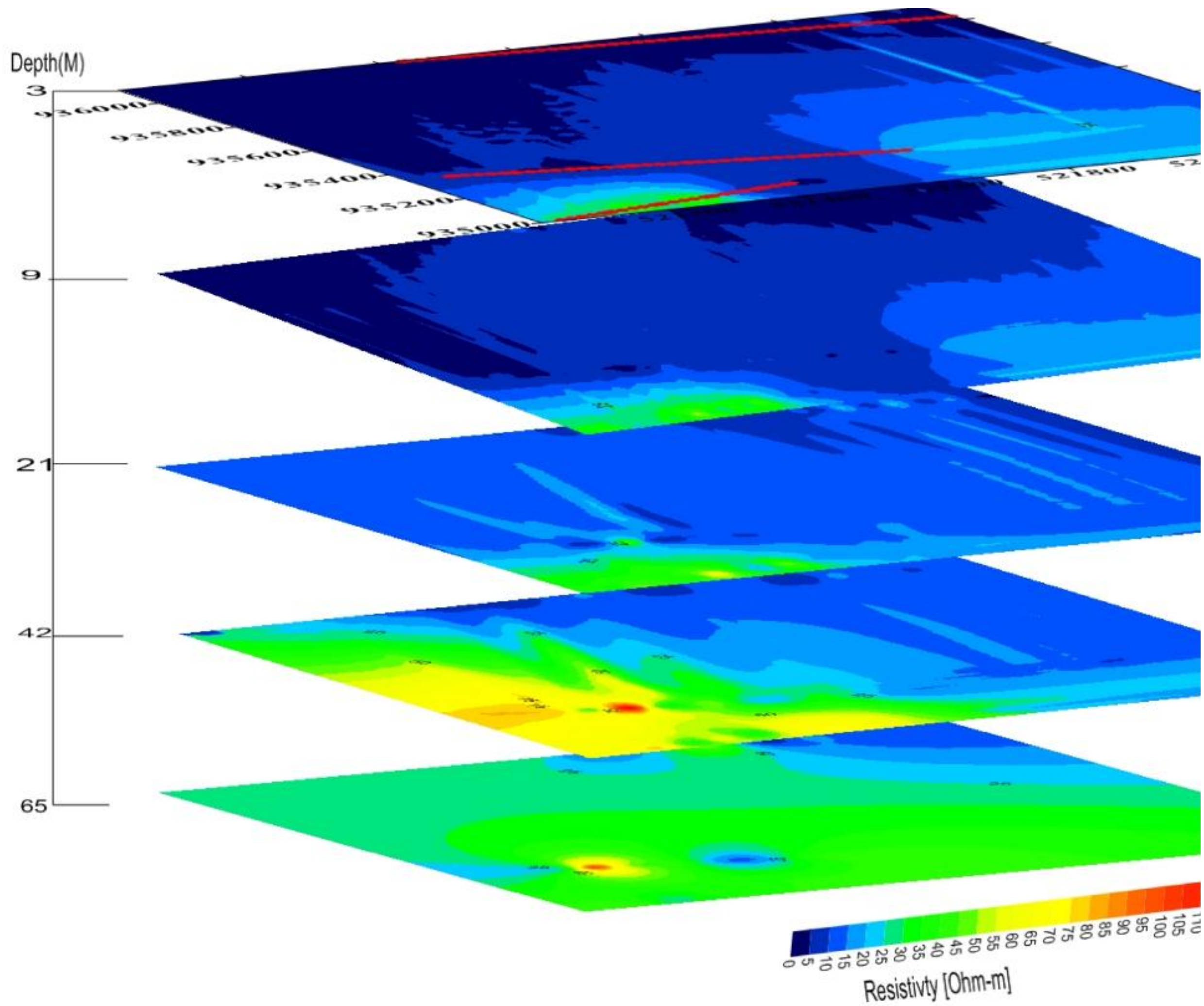

Figure 4.4 Sliced-Stacked plots of resistivity as a function of depth.

At shallow depths (3 to 9 m) the resistivity variation on the south eastern part shows relatively high resistive part of the ground. This area at shallow depth is covered with dry soil with no or less moisture content. Due to its distance from River Awash and with no apparent thermal manifestation in the form of springs the soil is dry and the resulting resistivity is relatively higher at shallow depth. Apart from this, the resistivity of the area increases with depth except at depths of about 42 m. As discussed in the interpretation of the individual resistivity imaging sections (section 4.1.1, figure 4.1), the depth below this is marked as the zone where the springs are recharging.

Overall, from the stacked plot it is seen that an extensive low resistivity region is mapped at depth which shows the presence of zones of fluid saturation, but not necessarily thermal fluids as suggested by the relatively higher resistivity from that resulting through a combination of thermal activity and presence of fluids.

It can be observed that the relatively high resistivity zone has general SW-NE trend encompassing all the active thermal springs. This relatively resistive portion could define a SW-NE trending tectonic line following the main tectonic SW-NE trending line of the Wonji Fault Belt. Surface geological maps of the prospect area show that intra rift acidic complex of the Gedemsa unit covers the high resistive part, whereas the low resistive vast portion is covered by alluvial and lacustrine deposits and marginal complex ignimbrite units (Boku-Tede and Keleta units). From the resistivity imaging sections and stacked map one can recognize that the alluvial deposit/ top soil cover, of which moisture and salinity, increases at depth going to the north.

4.2 Magnetic Data

Total field magnetic data were collected over random points and covering most of the areas over which the electrical imaging lines extend. A total of about 500 data points were gathered with a station spacing of 40-50 m. These data were then corrected for diurnal variations and unexpected data readings were removed from close examination of the data set. IGRF values for the base stations were then employed and removed from the data to obtain the magnetic anomalies. In the following sections the presentation (in the form of magnetic anomaly, analytical signal and upward continued magnetic maps) and interpretation of these corrected and reduced data are given.

It is well known that erratic and complex characteristics of magnetic maps make interpretation of magnetic data only qualitative. " Indeed, interpretation is something of a fine art." (Telford et al., 1990). However, magnetic maps are normally useful to the exploration because they are easy in field data collection and data processing. This makes them the most widely used geophysical technique, both as a very useful aid in regional mapping and for the direct location of ore bodies that have a distinct magnetic signature.

4.2.1 Magnetic Anomaly Map of Gergedi Thermal Springs

Shown in Figure (4.5) is the magnetic anomaly map of the study area produced by subtracting the IGRF value from the diurnal corrected data from the Gergedi thermal springs. The surveyed area is bounded by UTM coordinates 935005 and 936718 m Northing and 521023 and 522377 m Easting.

From the map it is observed that the field intensity values lie between -259-267nT, which is a quite large variation in the magnetic intensity, indicating variations in either lithology, degree of alteration or basement topography. These variations can be classified into distinctive regions. More specifically, as shown on the total magnetic intensity map (Figure 4.5), there are three different regions based on the magnetic intensity variations, which are possibly related to the presence of local and regional zones of weakness and discontinuities and also areas of varying degree of hydrothermal alteration of the rock units.

The positive anomaly region can be classified as high magnetic anomaly (region A) that could possibly be the responses from rocks which have high susceptibility. This high magnetic anomaly zone is trending in the SW to NNE direction following the regional fault pattern. The second zone is of relatively low magnetic anomaly of 0-60nT (region B), and this may arise due to rocks of low magnetic susceptibility that have resulted from alteration of the rocks. This region covers the middle section from west to east and also the south east portion of the map which is a transition zone between the positive high responses and the negative low responses. The third region (region C), which is mostly in the SSW direction and in the area around the current active springs of the map, is a region of negative anomalies likely resulting from recent high degree of alteration of the rocks. These three regions are discussed separately in the following.

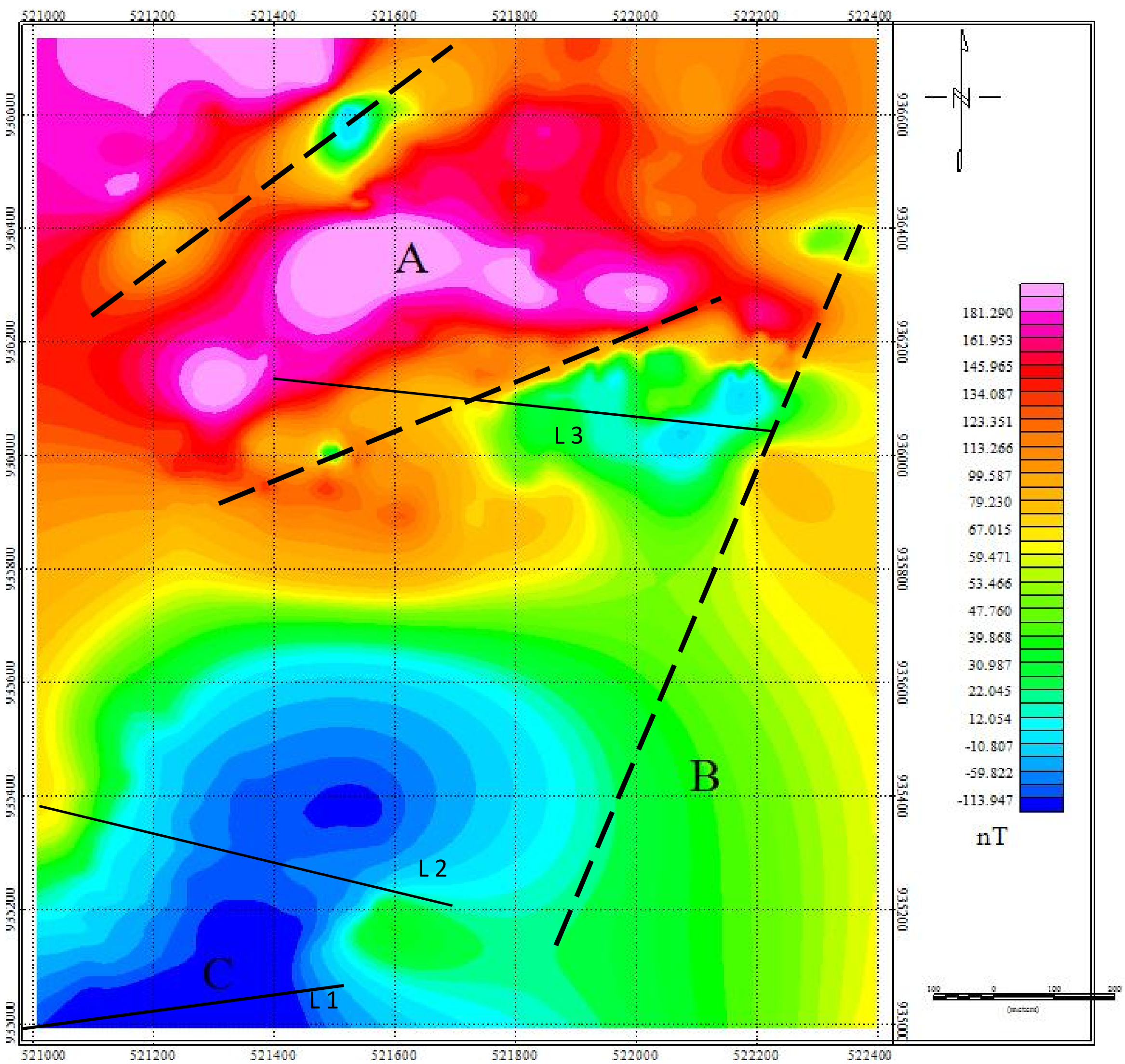

Figure 4.5 Magnetic Anomaly map of Gergedi thermal spring area. L1,L2 and L3 are resistivity imaging lines.

Region A

This high anomaly zone covering the region north of the area including River Awash has values ranging from 75- 267 nT. In this region, two week zones are mapped; the first weak zone runs from southwest to northeast part of the area. The second weak zone is south of the first and oriented nearly parallel to the first one. The second weak zone is crossed by the resistivity line (Line 3) and indicated at the imaging section (Figure 4.3). This high anomaly region in general and the weak zones in particular are trending following the general orientations of the Wonji Fault System. This is because of the fact that lineation in the magnetic contours usually follow regional geology or the prominent features of the area.

From the geological map (Figure 1.6) of the area, this high magnetic anomaly region is correlated with the ignimbrite and basaltic formations at the north and western regions respectively, whereas on the southern and eastern part the region is dominantly covered by alluvial deposits and rift floor complexes (Alula Damte et.al., 1992). Resistivity imaging Line 3 crosses this region and from the analysis of the resistivity section (Figure 4.3) the area is covered by relatively high resistive rocks down to depth. From the upward continued maps (Figures 4.8 and 4.9) the region shows the high magnetic anomaly continuing in depth. Therefore, the magnetic response of this region is from deep-seated rocks/materials, on the other hand no or little contribution for the anomaly responses from the shallower materials.

Region B

The surveyed area is characterized by a number of major short wavelength anomalies on the southern half and linear long wavelength anomalies mainly in the northern part of the survey area. The long wave length anomalies are the response of the rocks from the depth whereas the short wave length anomalies believed to be the response from the shallower features which disappeared in the upward continued maps. The region classified as Region B on the anomaly plot is the transition region between the positive high on the northern and the negative low region on the south western.

One of the weak zone determined at region **A** also crosses this region and are oriented following the regional trend it may be the structures shown in the geological map of the area (Alula Damte et al., 1992).

Region C

As an initial interpretation of the magnetic anomaly map, several thermally altered grounds cover the southwest region extending to the northeast of the area. The distribution of the hydrothermal manifestations is in agreement with the observed low anomaly trend indicated as Region C. This negative magnetic anomaly is clearly shown on the plot at the southwestern side of the surveyed area and is where the large discharge thermal springs are clustered. The low magnetic anomaly areas can be interpreted in terms of the responses from highly demagnetized subsurface rocks that have resulted from the hydrothermal alteration of the rock units. Besides the negative anomaly response could also be accounted to the alluvial and lacustrine deposits (Allula Damte et al., 1992), highly fractured rocks, and thermal alteration of the rock units. In the upward continued maps (Figure 4.8 and 4.9) this zone fades out at shallow depth and again the low magnetic anomaly region reappears as the magnetic data are further continued upward.

It is stated that magnetic structures do not occur at random, but are generally aligned along definite and preferred axes forming trends that can be used to define magnetic provinces (Affleck, 1963; Hall, 1979). Accordingly, the magnetic features that occurred in the study area in general and in this region in particular follow the prominent structural trends of the Wonji Fault Belt system that crosses the area as discussed for region A above.

4.2.2 Analytical Signal Map

Amplitude of analytic signal can be defined as the square root of the squared sum of the vertical and the horizontal derivatives of the magnetic field (Roest et.al., 1992), i.e.

$$|\mathbf{A}(\mathbf{x},\mathbf{y})| = \sqrt{\left(\frac{\partial M}{\partial x}\right)^2 + \left(\frac{\partial M}{\partial y}\right)^2 + \left(\frac{\partial M}{\partial z}\right)^2} \quad (4.1)$$

where A is the amplitude of the analytic signal and M is magnitude of the total magnetic field.

The analytical signal is formed through a combination of horizontal and vertical gradients of a magnetic anomaly and the method is very useful for delineating magnetic sources. The amplitude of a simple analytic signal peaks over magnetic contacts (Nabighian, 1972). Therefore, the procedure can also be used to find location of horizontal contacts and depths of magnetic contacts. The analytic signal has a form over causative bodies that depend on the locations of the bodies but not their directions of magnetization (Jeng et.al., 2003). This ‘filtering’ technique has a potential to reduce the ambiguity that could arise from the effect of a dipole source, particularly in low latitude areas, where reduction to pole is not effective but rather produces synthetic noise. However, if more than one source is present, then the shallow sources are well resolved but the deeper sources may not be well resolved. To avoid this limitation, taking analytic signal from upward continued data is preferred.

The analytic signal map of Gergedi Thermal springs area (Figure 4.5) is produced from the residual magnetic map of the plot and is shown in Figures 4. Close examination of the map confirms the existence of abnormal limiting/or bounding structures (anomaly peaks) on the southwestern side of the area, containing the active thermal springs, and also on the northern central part of the map. These lineaments/contacts are in correlation with the contacts that were determined using electrical imaging techniques.

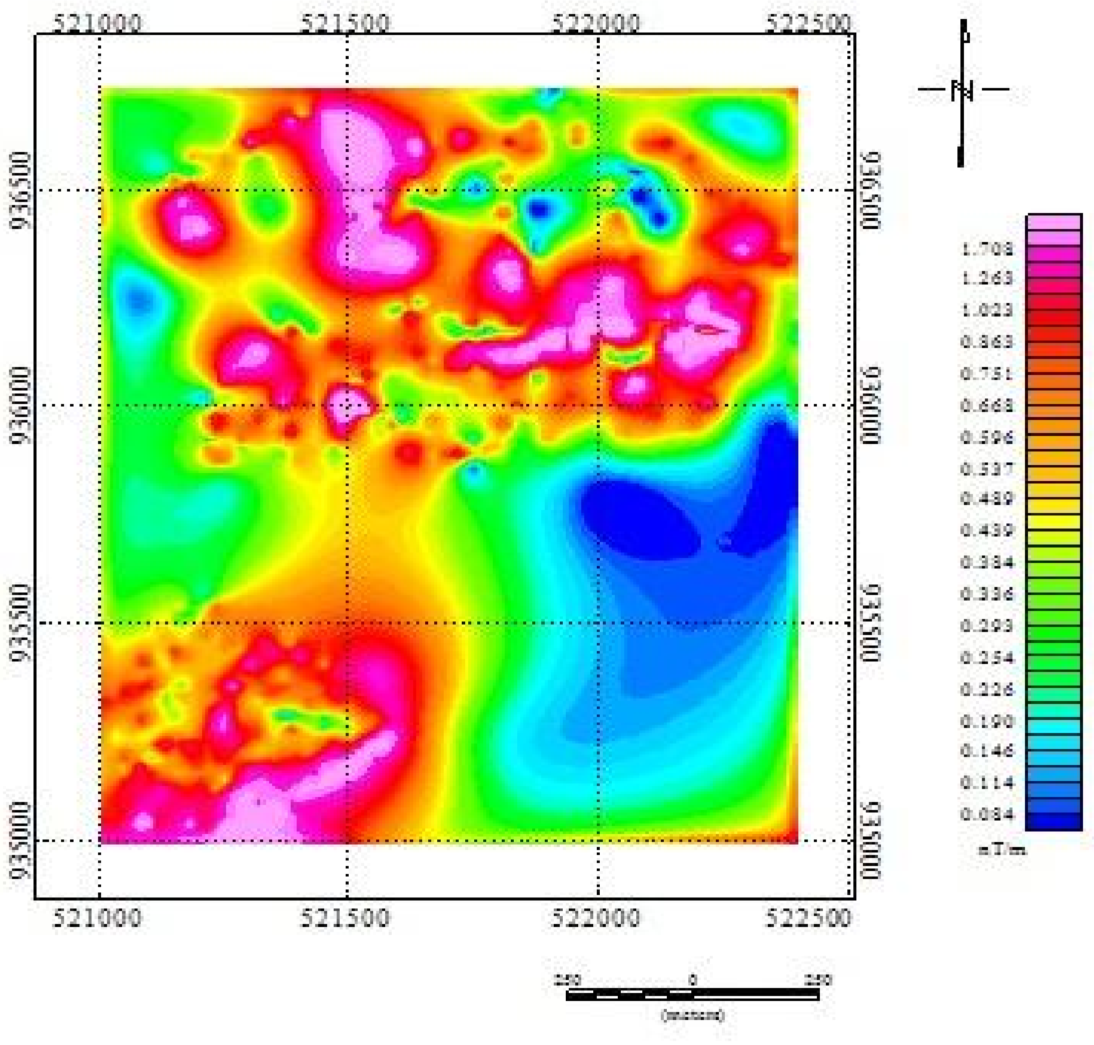

Figure 4.6 Analytic signal map of Gergedi area

4.2.3 Upward Continued Maps

The upward continued maps of the Gergedi thermal spring area are produced from the total magnetic intensity map. The anomaly map is continued to 100 and 300 m (and shown in Figure 4.8 and 4.9) to show the continuity of features of the map that has long wave length anomalies and it tends to suppress subtle features at the expense of longer wavelength anomalies.

Areas of very low magnetic anomaly are indicated on the north and north western sides of the study area and these are found to be different from the current thermal manifestation zones indicating the existence of potential zones for the production of thermal fluids.

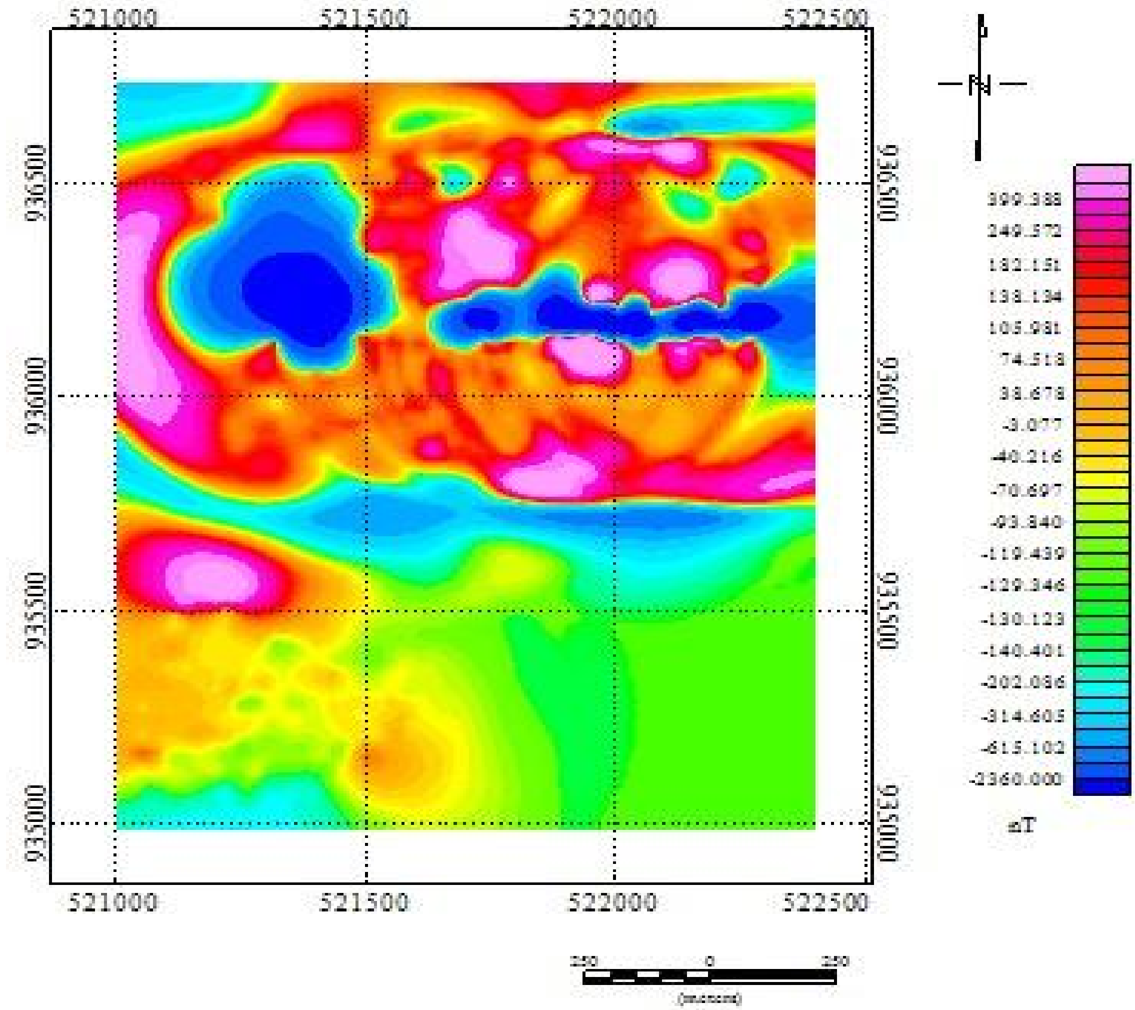

Figure 4.7 Upward continued map(up 100m) Gergedi thermal springs.

From these maps, it is seen that at upward continuation to 100 m and 300m two distinct aligned low magnetic areas are observed. These areas are extensive and cover the central part of the surveyed area. Similar low magnetic response reappears at the southwesten end and over the current active thermal spring of the area, although with smaller magntiude. In general these areas of low magnetic response at depth are expected to be potentail areas for the sinking of boreholes and extraction of thermal waters from a relatively shallower depth.

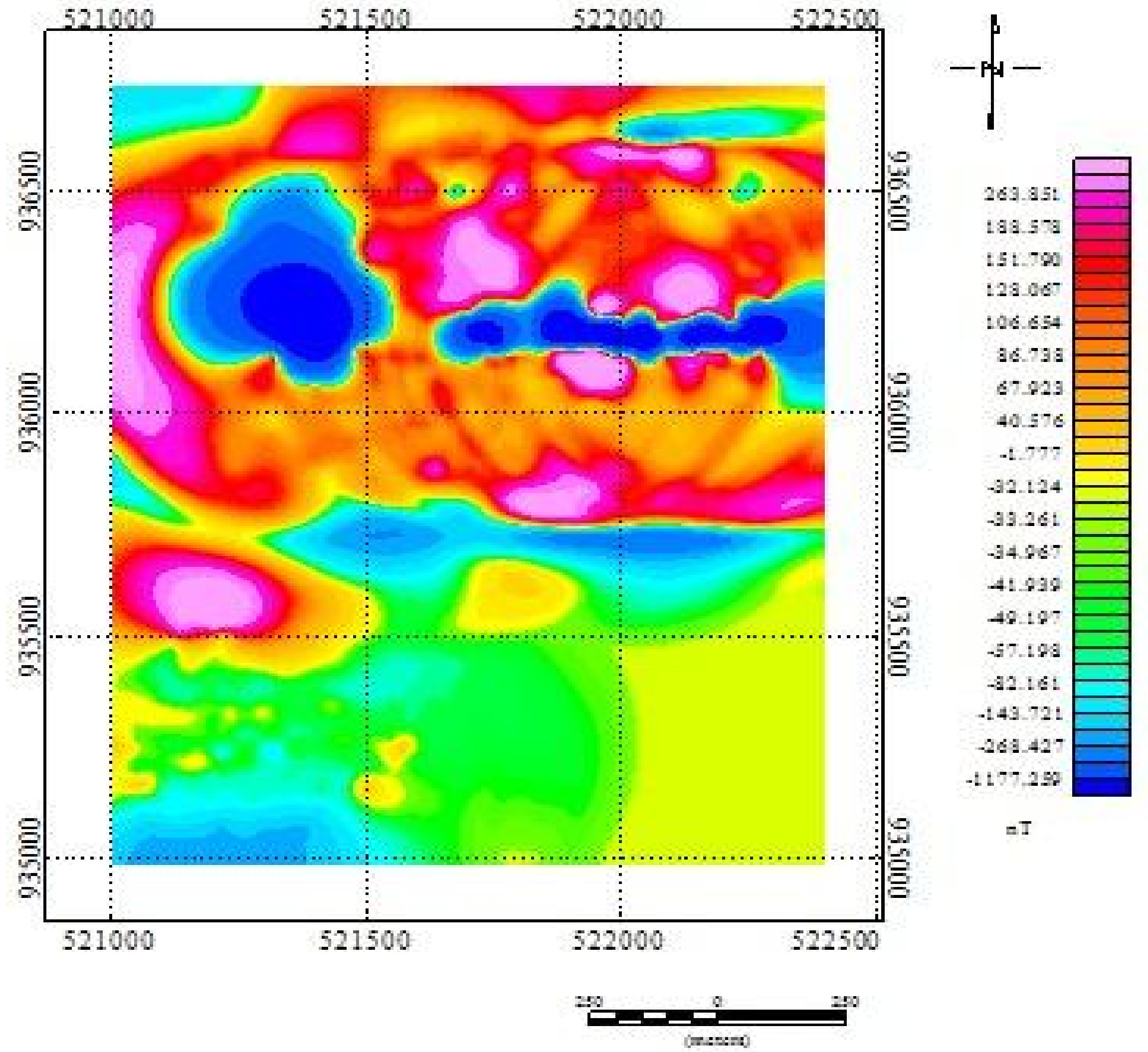

Figure 4.8 Upward continued (up 300m) map of Gergedi thermal spring area

Further upward continuation of the magnetic anomaly signal has shown that the areas of low magnetic response increase in their extent. This gain could be attributed to the effect of the thermal waters that have invaded the shallow regions of the subsurface and altered the insitu rocks.

CHAPTER FIVE

CONCLUSION AND RECOMMENDATION

5.1 Conclusions

2D electrical imaging and total field magnetic survey have been carried out on the Gergedi thermal springs, northwest of Wonji, in the Main Ethiopian Rift, to characterize the thermal setting and to map possible shallow weak zones that act as conduits for the discharging thermal fluids. It was also the objective of the survey to map and locate potential areas of shallow thermal water saturation. These methods have been found to be useful non-destructive geophysical methods for characterizing the subsurface conditions/images in many instances and have also been employed on the Gergedi thermal springs area. The methods, in association with geological, hydrogeological and structural information from other studies has been used to minimize the ambiguity of the geophysical analysis.

The resistivity imaging survey was carried out along three lines (Line-1 to Line-3); survey profiles selected such that the first line is traversing almost east to west straddling the current active thermal springs, the second line is parallel and north of the first line and the third line, which is again parallel to the first two lines, but is north of Awash River, a river that crosses the thermal spring area. Imaging data on the three profiles extended over a total length of about 2.5 km and total volume of 4600 data points. The total field magnetic data were collected over random points and covering most of the areas over which the electrical imaging lines extend. A total of about 517 data points were gathered with a station spacing of 40-50 m.

The 2D Resistivity imaging data were processed with the RES2DINV program whereas the magnetic data were processed with the Oasis Montaj software and in addition Surfer software also used to present the data. Hence, the imaging data are presented in the form of inverted true resistivity model sections, slice/stacked sections while the magnetic data were presented in the form of anomaly contour maps, analytical signal maps and upward continued maps and profile plots. Interpretations are thus drawn from these 2D resistivity imaging sections, resistivity stacked maps, total magnetic intensity, analytic signal and upward continued magnetic maps and profiles. These results of these interpretations are summarized below.

The interpretation of the 2D resistivity imaging sections show that the Gergedi thermal springs area has geoelectric layers with low, moderate and relatively high resistivity horizons that could possibly have resulted from moisturized saline top soil cover, ignimbrite and/or weathered basalt and rhyolite and/or weathered ignimbrite respectively. The resistivity imaging has also mapped different faults through which the geothermal fluids come to the surface along these fractures.

The possible potential aquifer zones are thought to be the highly fractured, water saturated ignimbrites. This formation could have high water yield.

The analysis of the magnetic data have shown the faults in addition to these detected by the resistivity imaging sections and it also revealed new potential sites of low magnetic response that can be used for further exploitation of the thermal resources. The magnetic method also mapped SW-NE expanding thermal alteration zones over the study area at shallower depth.

The application of the integrated geophysical method has facilitated the data interpretation and has greatly reduced the ambiguity inherent in each method. The results of the different geophysical methods have shown good correlation with each other, highlighting the merits of the use of integrated geophysical survey.

5.2 Recommendations

Based on the results obtained and the limitation of this research the following points are recommended.

The qualitative description of the magnetic data and the resistivity imaging data presented above is quite limited in areal coverage which is restricted only in the area where the maximum thermal manifestations occur. Therefore regional potential field data (Gravity and Magnetics) integrated with deep geophysical surveys using electromagnetic techniques, like Magneto Telluric (MT), are recommended to

- Elucidate the deep seated structure at the hot springs area. This also will highlight more information about the real situation and subsurface flow of the hot water.
- Adequate coverage of the area by gravity and magnetic data can provide additional information and as such facilitate complete understanding and in planning for future utilization of the resources.

Integrating the geophysical results with hydrogeological, geochemistry and heat flow model is helpful before qualifying the area for large-scale usage of geothermal resource.

Even though this study is not detail and the results are exhaustive to characterize the thermal area fully, from the results obtained it is possible to conclude that the thermal springs have reliable potential for small scale investments in areas of entertainments and thermal therapy. Potential areas other than the current active thermal springs are identified from the magnetic prospecting, thus additional possible heat bathes can be constructed where the magnetic lows are shown.

One of the most useful geological applications of magnetic survey is to map structural trends by following lineation in magnetic contours (Dobrine and Savit,1988). Therefore from this study geologists are recommended to re-sketch the detailed geological map of Gergedi thermal springs area.

References

Adepelumi,A.A.,Ako,B.D.,Ajayi,T.R.,Olurunfemi,A.O.,Awoyemi,M.O., and Falebita, D.E., (2008). Integrated Geophysical mapping of the Ifewara transcurrent fault system,Nigeria. *Journal of African Earth sciences*, **52**, 161-166.

Alula Damte, Boccaletti, M., Mazzuoli, R., Getaneh Assefa., Tortorici, L., (1992). Geological Map of the Nazareth Dera Region (Main Ethiopian Rift), Scale 1:50,000. S.E.L.C.A, Florence, Italy.

Ansari, A.H. and Alamdar, K., (2009). Reduction to the Pole of Magnetic Anomalies Using Analytic Signal, *World Applied Sciences Journal,* **7 (4),** 405-409.

Bhattacharyya, B. K., and Leu, L. K.,(1977).Spectral analysis of gravity and magnetic anomalies due to rectangular prismatic bodies. *Geophysics*, **42**, 41-50.

Byerly, P. E., and Stolt, R. H., (1977). Attempt to define the Curie point isotherm in Northernand Central Arizona: *Geophysics*, **42**, 1394-1400.

Dobrin, M.B. and Savit, C. H., (1988). Introduction to geophysical prospecting,fourth edition. McGraw-Hill, New York, USA .Pp498-613,750-837.

ELC, (1987). Geothermal Reconnaissance study of selected sites of the Ethiopian Rift System,(Geophysical report), Milano, Italia.

Geosoft, (2005). Oasis Montaj, Mapping and filtering software. Toronto, Canada, Geosoft incorporated.
Getaneh

Golden Software Inc. (2010). Surfer® 9, contouring and 3D surface mapping for scientists and engineers, Golden software, Inc. Colorado.

Grauch,V.J.S.,M.R. Hudson,and S.A Minor,(2001).Aeromagnetic expression of hydrgeologically important faults, Albuquerque basin, New Mexico SAGEEP, Denver Co.,USA

Griffiths D.H, Barker R.D., (1993). Two-dimensional resistivity imaging and modeling in areas of complex geology. *J. Appl. Geophysics*, **29**, 211–226.

Loke, M.H.**,** (1997, 1999, 2000). Electrical imaging surveys for environmental and engineering studies. A practical guide to 2-D and 3-D surveys.

Loke, M.H., and R. D. Barker,(1996) Rapid least-square inversion of apparent resistivity pseudo sections by quasi-Newton method. *Geophysical Prospecting*, **44**, 131-152.

Loke, M. H., (2000). Topographic modeling in electrical imaging inversion: 62nd Conference and Technical Exhibition, EAGE.

Boccaletti, M., Bonini, M.,Mazzuoli,R.,Bekele Abebe, Piccardi,L. ,Tortorici,L., (2008). Quaternary oblique extensional tectonics in the Ethiopian Rift (Horn of Africa). *Tectonophysics,* **287** ,97-116.

Mary, H. D and Mario F., (2004).what is geothermal energy? Istituto di Geoscienze eGeorisorse,CNR, Pisa, Italy, 1-61.
Available at http://www.geothermal-energy.org/314,what_is_geothermal_energy.html
Date accessed May, 2011.

Meseret Teklemariam.,Kibret Beyene., Yiheyis Amdeberhan, Zewde Gebregziabher, (2000). Geothermal development in Ethiopia. *proceedings world geothermal congress*. Kyush-Tohoku,Japan.

Mohr, P.A..(1983).Perspective on the Ethiopian volcanic province. *Bulletin of Volcanology*.**46**:23-44

Mohr, P. ,(1967). Major volcano-tectonic lineament in the Ethiopian Rift System. *Nature*, **213**, 664-665.

Mohr, P.A., (1962).The Ethiopian Rift System. *Bulletin of Geophysical Observatory* .Addis Ababa University, **5**, 33-62

Nabighian. M.N., (1972). The analytic signal of two-dimensional magneticbodies with polygonal cross section: its properties and use forautomated anomaly interpretation. *Geophysics,***37**,507-517.

Nicolas,O., Mariita a, G. Randy Keller b., (2007).An integrated geophysical study of the northern Kenya rift. *Journal of African Earth Sciences*, **48**, 80–94.Elsevier.

NOAA, (2011). National Oceanic and Atmospheric Administration.
http://csc.noaa.gov

SCHÖN, J. (1983). Petrophysik, Enke, Stuttgart.

Tadesse Mamo,(2002). Geothermal exploration in Ethiopia, country report, Geothermal division, Ethiopia geological survey, Addis Ababa, Ethiopia.

Tamiru Alemayehu and Tigistu Haile. (2008). Geophysical exploration of the Boku Geothermal Area, Central Ethiopian rift. *Geothermics*, **37**, 568-596.

Tamiru Alemayehu,(2003). Controls on the occurrence of cold and thermal springs incentral Ethiopia. *African Geosciences Review Journal,* **l9 (4),** 245-251.

Tamiru, Alemayehu., Vernier, A., (1997).Conceptual model for Boku hydrothermal area(Nazareth), Main Ethiopian Rift. *SINET: Ethiopia. J. Sci.,* **20(2)**, 283-291.

Telford, W.M., Geldart, L.P. and Sheriff, R.E., (1990).Applied Geophysics, 2nd Edition. Cambridge University Press, Cambridge, UK. Pp 6-48,522-562.

Theodros Solomon. (2008).Characterization of the Bullbula (Gergedi) thermal springs, Wonji, Main Ethiopian Rift, using integrated Geophysical Methods. Unpublished Msc Thesis.Addis Ababa University.

Tigistu Haile and Tamiru Alemayehu. (2010). Aquifer Characteristics thermal springs in the axial part of the Main Ethiopian Rift.

Tigistu Haile, Ranieri,G., Tamiru Alemayehu.(2003).Applicationof Geophysical methods for the evaluation of thermal centers and their structural controls in Boku, Nazareth, Main Ethiopian Rift. *Near Surface Geophysics*.

Tigistu Haile, Tamiru Alemayehu., Shimeles Fisseha. (2002). Geophysical Investigations of the Boku Thermal Springs, Nazareth. *SINET, Eth. J. Sci.* **25(2),** 253-262.